M-Pos479

SIMULATION OF TRANSLATIONAL AND ROTATIONAL DIFFUSION OF ANTHRACENE IN SOLUTION: INFLUENCE OF TEMPERATURE, AND VISCOSITY. ((**Gouri S. Jas**, Yan Wang, and Krzysztof Kuczera)) Department of Chemistry and Biochemistry, The University of Kansas, Lawrence, KS 66045. gouri@tedybr.chem.ukans.edu

Molecular dynamics (MD) simulations of 1 ns length were performed for anthracene in cyclohexane (at 284 K, 300 K, 314 K) and in 2-propanol (at 300 K). Rotational and translational diffusion parameters were calculated and compared with the hydrodynamic theory predictions, and with fluorescent anisotropy decay measurements. The computed translational diffusion coefficient of anthracene in cyclohexane and in 2-propanol agree more closely with the hydrodynamic theory of *slip* boundary than *stick* conditions. Translational diffusion coefficients along each molecular axis (X,Y,Z) are also computed. Computed rotational diffusion coefficients for anthracene in both solvents fall between stick and slip conditions. The time constant found in the second order correlation function along the direction of transition dipole moment (17 ps and 25 ps) agrees very closely with the measured decay time (16 ps and 25 ps). Influence of viscosity and temperature on translational and rotational diffusion coefficients are in good agreement with the hydrodynamic theory. The solvent structure around anthracene was analyzed to generate a microscopic picture of solvation.

M-Pos480

THE SIMULATION OF SUPERCOILED DNA DYNAMICS USING AN ELASTIC CONTINUUM MODEL.

((**T.P. Westcott**, J.A. McCammon)) Department of Chemistry & Biochemistry, University of California, San Diego, 9500 Gilman Drive, La Jolla, CA, 92093-0365

The main objective of this research is to understand and visualize the dynamics of supercoiled DNA. Since supercoiled DNA is hundreds, thousands, tens of thousands of base pairs or longer, traditional molecular dynamics cannot be used to simulate such DNA because it is not fast enough to treat such large DNA for long time scales. Thus, developing methods which can treat long DNA for long time scales is important. Classical continuum elasticity theory provides a good, yet simple model of DNA. Elastic rod theory is used to develop equations for DNA dynamics using arguments based upon the balance of forces and the balance of momentum at each cross section of the rod. The dynamical equations can include external forces such as electrostatic interactions, energy dissipation terms to account for viscous drag, and a random force to account for thermal fluctuations. It is also possible to study chains containing regions of intrinsic curvature, altered twist, differences in intrinsic bending and twisting stiffness, or bound drugs and/or proteins.

(Supported by Sloan-DOE Joint Postdoctoral Fellowship in Computational Molecular Biology).

CHANNELS (OTHER)

Tu-AM-A1

PERMEATION THROUGH THE CALCIUM RELEASE CHANNEL (*CRC*) OF CARDIAC MUSCLE ((D. Chen*, Le Xu†, A. Tripathy†, G. Meissner†, **R. Eisenberg***)) Dept's of Biophysics, *Rush Medical College, Chicago IL 60612 and †Univ. of North Carolina, Chapel Hill NC 27599.

Current voltage (*IV*) relations were measured from single open *CRC* channels in twelve KCl solutions, symmetrical and asymmetrical, from 25mM to 2M. *IV* curves are surprisingly linear, even at the extremes of voltage (±150mV≈6*kT/e*), even in asymmetrical solutions, e.g., 2M‖100mM. It is awkward to describe straight lines as sums of exponentials in a wide range of solutions and potentials and so traditional barrier models have difficulty fitting this data.

We have fit the data with the Poisson and Nernst Planck equations (PNP: J. Membrane Biology, *150:* 1–25, 1996) using adjustable parameters for the diffusion constant of each ion and for the effective density of fixed, i.e., permanent charge $P(x)$ along the channel's 'filter' (7Å diameter, 10Å long). If $P(x)$ is described by just one parameter (i.e., $P(x) = -4.2$M independent of x), the fits are satisfactory (*RMS* error/*RMS* current = 6.4/67, pA/pA). If $P(x)$ is described by 4 parameters, the fit is significantly better (5.8/67), and the parameter values are reasonable, $P(x) = -4.8 + 8.1J_0(\pi x) - 4.1J_0(2\pi x) - 9.9J_0(3\pi x)$ (in Molar, where x is the (normalized) location in the channel; J_0 is a Bessel function of order zero) and diffusion constants in the pore, $D_K = 1.5\times10^{-6}$, $D_{Cl} = 4.1\times10^{-6}$ cm^2/sec.

Because the fixed charge density of *CRC* is so high, and the filter so small (in PNP's view of the channel's pore), the concentration of ions in and near the filter have a large effect on the potential profile and permeation. The change in the shape of the potential profile from solution to solution predicted by PNP is thus large, often more than *kT/e*.

This work was supported by NSF and NIH grants.

Tu-AM-A2

PERMEATION THROUGH PORIN AND ITS MUTANT G119D. ((J. Tang*, D. Chen*, N. Saint†, J. Rosenbusch†, **R. Eisenberg***)) *Dept of Biophysics, Rush Medical College, Chicago IL 60612 and †Biozentrum, Basel, Switzerland.

Current voltage (*IV*) relations were recorded from single open channels of *OmpF* (wild type) porin and its mutant *G119D* that has one additional negative charge (aspartate) in its constriction site. Measurements have been made so far in eight KCl solutions, symmetrical and asymmetrical, from 3M to 10 mM in the voltage range ±200mV ≈ 8*kT/e*.

IV curves were fit with the Poisson and Nernst Planck equations (PNP) using adjustable parameters to describe the diffusion constant of each ion and the effective density of fixed, i.e., permanent charge $P(x)$ lining the channel's pore. Pore dimensions are taken from the known structure of the channel proteins. Fits to data are satisfactory if $P(x)$ is described by three parameters. PNP is able to fit a wide range of *IV* relations because the shape of the potential profile along the channel changes with solution, as it must in any self-consistent theory.

PNP is an approximate theory that ignores almost all the complexity of porin structures seen by crystallography, and describes the protein by effective, not real parameters. Thus, it is surprising that even our first fits of PNP to the *IV* data give nearly the ideal result, within ±15%, *net charge* $= \int [P(x;OmpF) - P(x;G119d')]dx = -1e$. (Fits to data from *OmpF* and *G119D* were done independently and parameter values were not adjusted in any way.)

Evidently, changes in the actual charge of the protein can be well described by changes in the effective profile $P(x)$. It is important to see how well PNP predicts *IV* relations of other mutants, and how well the charge distribution $P(x)$ describes the spatial average of the real (three-dimensional) charge distributions of those mutants, as determined by crystallography.

Tu-AM-A3

CURRENTS THROUGH SINGLE CHANNELS OF MALTOPORIN. ((J. Tang*, N. Saint†, J. Rosenbusch†, **R. Eisenberg***)) *Dept of Biophysics, Rush Medical College, Chicago IL 60612 and †Biozentrum, Basel, Switzerland.

Maltoporin is a trimeric channel protein, whose structure is known at 2.7Å resolution, containing three adjacent narrow pores, 4.5Å in diameter. Each pore has a 'greasy slide' and 'ionic track' that allow rapid diffusion with considerable selectivity.

Single trimers insert into azolectin bilayers and their pores show cooperative gating, as expected from the structure. The voltage dependence of gating is qualitatively similar to, but quantitatively different from *OmpF* porin: more voltage (and time) is needed to start maltoporin's much slower 'open/then close' behavior. Fig. 1 shows current in 1M KCl solutions after a 280mV step. Fig. 2 shows the finely curved current–voltage relation of a trimer with 3 open channels. The chord conductance is ~400 pS, compared to ~4 nS for *OmpF* under the same conditions.

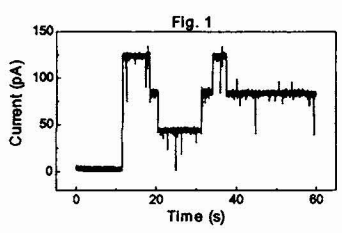

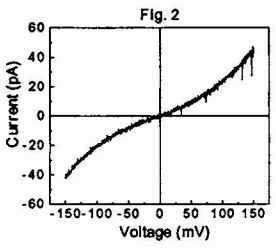

Tu-AM-A4

WHERE IS THE RATE-LIMITING STEP IN PERMEATION THROUGH VOLTAGE-GATED PROTON CHANNELS? ((**T.E. DeCoursey** and V.V. Cherny)) Dept. Mol. Biophys. & Physiology, Rush Medical Center, Chicago, IL

The proton conductance (g_H) of voltage-gated H^+ channels is 10-100 fS near physiological pH (Byerly & Suen, 1989, *J.Physiol.* 413:75; D&C, 1993, *Biophys.J.* 65:1590). Between pH_i 7.5-5.5 g_H increases only ~1.8/Unit (D&C, 1995, *J.Physiol.* 489:299-307). In contrast, g_H of gramicidin and other channels increases 10-fold/Unit decrease in pH, between pH 4-0, consistent with diffusion being rate-limiting. The effects of substituting deuterium, D_2O, for water, H_2O, on the voltage-activated H^+ conductance of rat alveolar epithelial cells were studied. D^+ carried current through proton channels, but g_H was ~twice as large in H_2O as in D_2O. D_2O reduced g_H more than could be accounted for by bulk solvent properties- the mobility of H^+ is only 41% greater than D^+ (Lewis & Doody, 1933, *J.Am.Chem.Soc.* 55:3504). This result suggests that the rate-limiting step in permeation occurs in the channel rather than in the diffusional approach and that D^+ interacts specifically with the voltage-gated H^+ channel during permeation. The g_H is evidently near saturation at neutral pH, seven orders of magnitude lower [H^+] than where saturation occurs in gramicidin (Akeson & Deamer, 1991, *Biophys.J.* 60:101). This result also strengthens the hypothesis that H^+ (D^+) and not OH^- (OD^-) is the ionic species carrying current.

Support: NIH grant HL52671, American Heart Association Grant-in-Aid.

Tu-AM-A5

VOLTAGE-INDUCED SLOW ACTIVATION OF MECHANO-SENSITIVE CHANNELS IN THE ABSENCE OF APPLIED STRETCH. ((**Shai D. Silberberg*** and Karl L. Magleby**)) *Department of Life Sciences, Ben-Gurion University of the Negev, Beer-Sheva, 84105, Israel and **Department of Physiology and Biophysics, University of Miami School of Medicine, Miami Florida 33101 USA.

Mechano-sensitive (MS) channels activate rapidly with stretch (within ms) and also deactivate rapidly when the stretch is removed. Although some MS channels are also modulated by voltage, there is little information on the time course of the voltage-induced activation. Using the patch clamp technique, we observed that the predominant MS channels in *Xenopus* oocytes had an uncommonly slow response to step changes in voltage in the absence of applied stretch. Following a step from -50 to +50 mV, MS channels activated after a delay of up to tens of seconds, and upon repolarization, the channels deactivated with a time course of seconds. There appeared to be cooperativity in the delay to activation among channels, raising the possibility that some common factor controls the delayed activation. The delay was prolonged by holding at more negative potentials or by applying a brief stretch prior to the depolarization. At +50 mV, a brief stretch applied during the delay rapidly activated the channels, which then remained activated for the duration of the depolarization. In contrast, applying a brief stretch during a voltage-induced slow deactivation at -50 mV terminated channel activity upon release of the stretch. These observations suggest that, when activated by voltage, the MS channel is in a different functional gating configuration than when it is activated by stretch, and that the channel can inter-convert between these gating configurations. Grants: *US-Israel BSF, *Israeli MSA, **NIH, and **MDA.

Tu-AM-A6

THE MECHANOELECTRICAL-TRANSDUCTION CHANNEL OF THE BULLFROG'S SACCULAR HAIR CELL IS HIGHLY Ca^{2+}-SELECTIVE. ((**Ellen A. Lumpkin**, Robert E. Marquis, and A. J. Hudspeth)) Howard Hughes Medical Institute and Laboratory of Sensory Neuroscience, The Rockefeller University, New York, NY 10021 (sponsored by S. N. Burlacu).

The mechanoelectrical-transduction channel of the hair cell is permeable both to monovalent cations, such as the K^+ that normally bears most of the transduction current, and to divalent cations. Ca^{2+} serves as a feedback signal in the adaptation process that sets the transduction channels' open probability; an understanding of adaptation therefore requires that the magnitude of Ca^{2+} influx be defined. Because transduction channels are more permeable to Ca^{2+} than to Na^+ and K^+, however, the amount of current carried by Ca^{2+} cannot simply be inferred from its mole fraction.

To determine the Ca^{2+} current through transduction channels, we made transepithelial voltage-clamp recordings to measure extracellular receptor currents in response to otolithic-membrane displacement. The apical surface of a saccular macula was bathed with solutions in which the mole fractions of Na^+ and Ca^{2+} were varied or with those in which either Na^+ or Ca^{2+} served as the sole permeant cation. The receptor currents in test solutions were normalized to the values recorded in standard saline solution containing the permeant cations 110 mM Na^+, 2 mM K^+, and 4 mM Ca^{2+}. To minimize the effects of other ionic conductances, the cells were depolarized by bathing the basolateral epithelial surface in high-K^+ perilymph.

In the absence of Na^+, 4 mM Ca^{2+} supported a receptor current 25% as large as that in standard saline solution. Although the channels were not passing maximal current, the response in 24 mM Ca^{2+} was 90% that in 24 mM Ca^{2+} plus 56 mM Na^+; Na^+ thus bore a small fraction of the current in the presence of Ca^{2+}. In mixtures of Na^+ and Ca^{2+}, the response displayed an anomalous mole-fraction effect.

These results confirm that, like voltage-gated Ca^{2+} channels, the hair cell's transduction channel is highly selective for Ca^{2+} over Na^+. The data also indicate that this channel's pore may contain more than one cation-binding site.

This research was supported by H H M I and by N I H grant DC 00241.

Tu-AM-A7

ION CHANNELS FROM INFLUENZA VIRUSES:- MOLECULAR DYNAMICS SIMULATIONS OF M2 AND NB CHANNEL MODELS.
((**M.S.P. Sansom***, R. Bull*, A. Premkumar* and G. Ewart*)) *Lab. of Molecular Biophysics, University of Oxford, Oxford, U.K. & *JCSMR, Australian National University, Canberra, Australia.

The M2 protein from influenza A virus forms proton permeable ion channels which are activated by low pH. The NB protein from influenza B also forms ion channels, permeable to monovalent cations. Both proteins are small (≤ 100 residues) and each contains a single transmembrane (TM) helix. Channels are thought to be formed by assembly of protein oligomers to yield parallel bundles of TM helices surrounding a central pore. Restrained MD simulations, run *in vacuo* using a simulated annealing protocol, have been used to generate models of transbilayer pores formed by bundles of TM helices from M2 or from NB. These models have been refined by 1 ns duration MD simulations with TIP3P water molecules within and at the mouths of the pore, and with a simple hydrophobic potential to mimic a lipid bilayer. The resultant models have been analyzed in terms of their pore geometries and predicted single channel conductances. Numerical solutions of the Poisson-Boltzmann equation have been used to determine electrostatic potential energy profiles along each pore. The structure and dynamics of water molecules within the pores have also been analyzed. For channels formed by M2, models with residue His-37 in either a protonated or in a deprotonated state have been compared. The protonated state of the channel appears to be the 'open' form of the channel whilst the unprotonated form is 'closed'. In the protonated, 'open' form a continuous network of H-bonded water molecules extends along the entire length of the channel lumen, whereas in the deprotonated, 'closed' form the column of water molecules is interrupted in the vicinity of the ring of His-37 sidechains. This provides the basis of a plausible model for the gating of the M2 channel by lowered pH.

Tu-AM-A8

THE ACTIVE OLIGOMERIC STATE OF THE INFLUENZA VIRUS M_2 ION CHANNEL IS A TETRAMER ((L.H. Pinto*, Q. Tu*+, T. Sakeguchi+, C. Gandhi* and R.A. Lamb+#)) Dep'ts of *Neurobiology & Physiology and +Biochemistry, Molecular Biology & Cell Biology and #Howard Hughes Medical Institute, Northwestern University, Evanston, IL 60208

The influenza A virus-associated M_2 ion channel is thought to function by acidifying the virion interior and equilibrating the pH gradient across the *trans* Golgi network in the infected cell, and the M_2 protein forms a tetramer when examined on SDS-PAGE under non-reducing conditions. However, a higher order molecular form is sometimes observed and thus it is necessary to determine the active form of the molecule. This was done by studying the currents of oocytes that expressed mixtures of the wt M_2 protein and the mutant protein M_2-$V_{27}S$ which is resistant to the inhibitor amantadine. The composition of mixed oligomers of the two proteins expressed in individual oocytes was examined after adding an epitope tag to the wt M_2 protein and it was found that the subunits mixed freely. When the ratio of wt to mutant protein subunits was 0.85: 0.15, the amantatine sensitivity was reduced to 50% and for a ratio of 0.71:0.29 to 20 %. These results are consistent with the amantadine-resistant mutant being dominant and the oligomeric state being a tetramer

CARDIAC ELECTROPHYSIOLOGY I

Tu-AM-B1

OVER-EXPRESSION OF NERVE GROWTH FACTOR (NGF) ALTERS ION CHANNEL ACTIVITY IN ADULT MOUSE HEART. ((B. Heath, J.Xia, A. Brooks*,H.J. Federoff,* and R.S. Kass)) Dept. of Pharmacology, Columbia University, New York, NY 10032 and *Depts of Neurology and Microbiology, University of Rochester, Rochester, NY 14642.

Single myocytes were isolated by Langendorff perfusion from the ventricles of wild type (WT) and transgenic adult mice (male DBA2 20-30g) which overexpress NGF in cardiac tissue (MHC-NGF: Hassankhani et al., 1993, 1995). K^+ and Ba^{2+} (L-type channel) currents were studied using whole cell patch clamp. Cells were clamped at -40 mV to inactivate I_{Na} , and K^+ currents were studied in the presence of nisoldipine (500 nM) to block L-type Ca^{2+} current. Extracellular solutions contained 1 mM Ba^{2+} to study L-type Ca^{2+} channel currents. All recordings were at room temperature. K^+ currents were activated by step depolarizations of 1 s duration to a series of potentials (-20 to +60 mV) applied at 0.1 Hz and I_{Ba} by 20 ms depolarizations applied at 0.2 Hz. Recording disclosed at least three differences: (1) during depolarization transient outward currents displayed slower activation and inactivation kinetics in MHC-NGF myocytes (n=3; see figure); (2) outward tail currents that could be blocked by 5 μM E4031 (a selective blocker of the rapidly activating component of the delayed rectifier) in WT myocytes (having a $V_{1/2}$ of activation of -4 ± 4 mV and slope factor of 13 ± 2 mV (n=4)) were not apparent in MHC-NGF cells; and (3) peak I_{Ba} density was greater in WT (7.9 ± 1 pA/pF (n=10)) than in MHC-NGF (2.8 ± 0.7 pA/pF (n=6)) myocytes with no marked changes in voltage-dependence or kinetics. These data are consistent with a down-regulation of expression of L-type channels and an E4031-sensitive current in adult NGF mice.

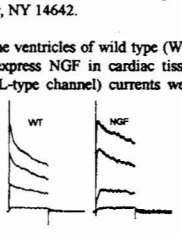

Tu-AM-B2

CHOLINERGIC REGULATION OF L-TYPE Ca^{2+} CURRENT ($I_{Ca,L}$) AND NITRIC OXIDE SIGNALING IN CAT ATRIAL MYOCYTES.
((**S.L. Lipsius**, C. Rechenmacher and Y.G. Wang)) Loyola University Medical Center, Dept. of Physiology, Maywood, IL 60154 (Spon. by K. Byron)

In atrial myocytes, 1 μM acetylcholine (ACh) inhibits $I_{Ca,L}$ and withdrawal of ACh elicits rebound stimulation of $I_{Ca,L}$. We used a perforated patch whole-cell voltage clamp technique to determine whether ACh-induced regulation of $I_{Ca,L}$ is mediated via nitric oxide (NO) signaling. Histochemical staining suggests that cat atrial myocytes express NO synthase activity. NO-generating compounds SIN-1 (100 μM), SNAP (1 μM) and sodium nitroprusside (SNP;10 mM) elicited an 88%, 83% and 96% increase in basal $I_{Ca,L}$ amplitude, respectively. ODQ (10 μM), an inhibitor of soluble guanylate cyclase (sGC), abolished the effects of each compound on $I_{Ca,L}$. Zaprinast (100 μM), an inhibitor of cGMP-specific phosphodiesterase, increased basal $I_{Ca,L}$ by 22% and enhanced the stimulatory effect of SNAP by 20% (N=6). On the other hand, ODQ failed to affect the inhibitory or rebound stimulatory effects of 1 μM ACh on $I_{Ca,L}$. Zaprinast had no affect on ACh-induced inhibition of $I_{Ca,L}$ and attenuated by 75% the rebound stimulation of $I_{Ca,L}$ elicited by withdrawal of ACh (N=4). L-NMMA (100 μM) decreased basal $I_{Ca,L}$ amplitude and prevented both the inhibitory and stimulatory effects of ACh. Addition of 5 mM arginine to L-NMMA restored basal $I_{Ca,L}$ and ACh-induced inhibition of $I_{Ca,L}$ but rebound stimulation of $I_{Ca,L}$ remained blocked. We conclude that ACh-induced inhibition and rebound stimulation of $I_{Ca,L}$ are not mediated via stimulation of NO/sGC signaling. However, constitutive NO may be prerequisite for ACh-induced regulation of basal $I_{Ca,L}$, possibly by maintaining endogenous cAMP levels in cat atrial myocytes. *Support by NIH grant HL27652*

Tu-AM-B3

GENISTEIN ELICITS A BIPHASIC RESPONSE OF L-TYPE Ca^{2+} CURRENT IN CAT ATRIAL MYOCYTES. ((**Y.G. Wang** and S.L. Lipsius)) Loyola University Medical Center, Dept. Physiology, Maywood, IL 60154

A perforated-patch whole-cell voltage clamp recording method was used to determine the effects of the tyrosine kinase inhibitor, genistein (GEN), on L-type Ca^{2+} current ($I_{Ca,L}$) in cat atrial myocytes. Within seconds of exposure, 50 μM GEN decreased $I_{Ca,L}$ by -54±8% below control (N=14). Over the next 1 min. of GEN exposure, $I_{Ca,L}$ increased by +32±11% above control. After 2 min. of GEN exposure, washout of GEN elicited a further, rapid increase in $I_{Ca,L}$ of 180±44% above control. $I_{Ca,L}$ returned to control levels within 2 min. of removing GEN. Daidzein (50-100 μM), a weakly active analog of GEN, elicited small inhibition or stimulation of $I_{Ca,L}$ and failed to further stimulate $I_{Ca,L}$ when removed. The biphasic effects of GEN on $I_{Ca,L}$ were qualitatively similar in cat ventricular myocytes although quantitatively much smaller. In atrial myocytes, the biphasic response of $I_{Ca,L}$ to 50 μM GEN was unaffected by 4 μM H-89, a protein kinase A (PKA) inhibitor; 2 μM chelethrin, a protein kinase C (PKC) inhibitor; 1 μM ryanodine; 100 μM L-NMMA, a nitric oxide (NO) synthase inhibitor or 3 μM ODQ, a soluble guanylate cyclase (sGC) inhibitor. These results suggest that basal $I_{Ca,L}$ is strongly modulated by tyrosine kinase activity. The biphasic effects of GEN on $I_{Ca,L}$ are not mediated via secondary signaling via PKA, PKC, NO/sGC or SR Ca^{2+} release. *Supported by NIH grant HL27652.*

Tu-AM-B4

REDUCED L-TYPE Ca^{2+} CURRENTS IN VENTRICULAR MYOCYTES ISOLATED FROM ENDOTOXEMIC GUINEA PIGS ((**J. Zhong**, T-C. Hwang, H.R. Adams, L.J. Rubin)) University of Missouri, Columbia, MO 65211. (Spon. by C.D. Hardin)

Septic shock resulting from gram-negative bacteria remains the most common cause of death in the intensive care units in the USA. The circulatory systems response to sepsis and its experimental counterpart, endotoxemia, includes a profound dysfunction in myocardial contractility, which is intrinsic to the myocyte and involves decreased systolic Ca^{2+} availability. We explored the possibility that L-type Ca^{2+} currents were reduced in ventricular myocytes isolated from guinea pigs four hours following an intraperitoneal injection of *E. coli* endotoxin (LPS, 4mg/Kg). Whole-cell patch clamp revealed that peak I_{Ca} density of LPS myocytes (3.5 ± 0.2 pA/pF) was significantly smaller than that of control myocytes (6.1 ± 0.3 pA/pF, $p < 0.05$) when the membrane potential was stepped from -40 mV to 10 mV. Correlated with reduced peak I_{Ca} was significantly shorter action potential durations of LPS myocytes (time to 50% repolarization: LPS, 314 ± 23 ms; control, 519 ± 36 ms, $p < 0.05$). When Ca^{2+} was substituted with Ba^{2+} as the charge carrier, peak I_{Ba} density of LPS myocytes remained significantly reduced (LPS, 7.3 ± 0.5 pA/pF; control, 11.3 ± 0.8 pA/pF, $p < 0.05$). The reduction in peak I_{Ca} density of LPS myocytes was not attributable to altered current-voltage relationship, steady state inactivation relation or a delay in recovery of I_{Ca} from inactivation. Isoproterenol, but not Bay K 8644, reversed the LPS-induced reduction of peak I_{Ca} (LPS, 10.2 ± 1.2 pA/pF; control, 12.6 ± 1.7 pF/pA, $p > 0.05$). In addition, isoproterenol reversed the LPS-induced decrease in cell contraction and systolic Ca^{2+} transient of myocytes isolated from the same LPS animal model. These data indicate that the function and/or regulation of L-type Ca^{2+} channels of ventricular myocytes are altered during endotoxemia, and the reduced I_{Ca} may contribute to the reduced systolic Ca^{2+} transient and myocardial dysfunction of endotoxemic animals.

Tu-AM-B5

FUNCTIONAL EXPRESSION OF THE AMPHIBIAN CARDIAC Na^+-Ca^{2+} EXCHANGER. ((Y.M. Shuba, V.G. Naidenov, K. Sandberg and **M. Morad**)) Department of Pharmacology, Georgetown University, Washington, DC 20007.

Na^+-Ca^{2+} exchanger is one of the major sarcolemmal Ca^{2+} transporter of cardiac myocytes. In frog ventricular myocytes Na^+-Ca^{2+} exchanger is regulated by isoproterenol via β-adreno-receptor/adenylate-cyclase/cAMP-dependent pathway providing a molecular mechanism for the relaxant effect of the hormone in the frog heart. Na^+-Ca^{2+} exchanger from the frog heart, fNCX1a, has recently been cloned and its primary structure has been determined (Iwata *et al., Ann. NY Acad. Sci.* 779:37, 1996). The clone includes 962 amino acids with 11 putative trans-membrane domains and 89.3% overall identity to the dog NCX1 isoform. fNCX1a, in addition, contains a nine amino acid insertion comprising a Walker A type putative nucleotide binding domain in the main cytoplasmic loop. To allow functional expression in *Xenopus* oocytes the 3'-untranslated region of the original fNCX1a clone was replaced with that of Na^+-glucose co-transporter clone pMJC424 (Hediger *et al., Nature* 330:379, 1987) which includes a poly(A) $^+$ tail. In addition, we replaced G for C in -3 position of fNCX1a to conform for a Kozak consensus initiation site. Injection of cRNA derived from modified fNCX1a cDNA resulted in the expression of the exchanger activity in *Xenopus* oocytes. The expression was examined by direct recording of the fNCX1a-induced membrane current (I_{Na-Ca}) using a glass funnel technique (Shuba *et al., Pflüg. Arch* 432:562, 1996) that permits intracellular perfusion of the oocytes as well as by measuring Na^+-dependent Ca^{2+} uptake of Na^+-loaded oocytes injected with Ca^{2+}-specific photoprotein, aequorin. Electrophysiological recording in Cl'-free intra- and extracellular solutions showed large I_{Na-Ca} in response to changes of membrane potential which could be reversibly blocked by millimolar concentration of Ni^{2+} and Cd^{2+}. I_{Na-Ca} induced by fNCX1a but not by NCX1 was strongly suppressed by membrane permeable isoforms of cAMP suggesting that regulation by β-agonists in native frog ventricular myocytes is an intrinsic property of the exchanger molecule. *Supported by NIH HL16152 and AHA Washington, DC Affiliate.*

Tu-AM-B6

A NEW CARDIAC SODIUM CURRENT COMPONENT IN RAT VENTRICULAR CELLS. ((**L. Goldman**, R. Aggarwal, S.R. Shorofsky and C.W. Balke)) Sch. of Medicine, Univ. of Maryland, Baltimore, MD 21201.

Rat ventricular cells express a tetrodotoxin (TTX) blockable Ca current, I_{Ca}(TTX), (Thomas, Balke and Shorofsky, Biophys. J., 68:A179, 1995). We find Na channels that are functionally distinct from classical cardiac Na channels carry this current. Freshly isolated adult rat ventricular cells were studied with whole cell patch clamp. I_{Ca}(TTX) and I_{Na} were isolated by TTX subtraction. L-type I_{Ca} was blocked with 10μM La. I_{Ca}(TTX) is insensitive to the Ca channel blockers Ni (50μM) and La (10μM), but is blocked nearly totally by 10μM TTX. I_{Ca}(TTX) channels are Na permeable. The I_{Ca}(TTX) conductance-voltage relation, g(V), was well described by a single Boltzmann, $g(V)=g_{max}/(1+\exp((V-V_{1/2})/k))$, ($g_{max}$:maximum conductance, $V_{1/2}$:potential for g(V)=1/2 g_{max}, k: slope factor). g(V) in both Na and Ca was better described as a sum of two Boltzmanns. In one cell in 3mM $[Ca]_o$, and no $[Na]_o$, $V_{1/2}$ was -47.6mV and k was -4.0mV. g(V) in 3 mM $[Ca]_o$ now with 1 mM $[Na]_o$ was fitted with the sum of a nearly identical ($V_{1/2}$:-49.2mV, k:-3.4mV) and a clearly distinct ($V_{1/2}$:-40.8mV,k:-2.1mV) component. I_{Ca}(TTX) activates over more negative potentials than the classical cardiac I_{Na}. In this cell, g_{max} ($V_{1/2}$ of -49.2 mV component) in 3 $[Ca]_o$, 1 $[Na]_o$ was 29.6% greater than in 3mM $[Ca]_o$ alone (mean increase:23.7%; 3 cells). Steady state inactivation in I_{Ca}(TTX) develops over more negative potentials ($V_{1/2}$:-79.9mV, k:8.3mV in 3mM $[Ca]_o$, O$[Na]_o$; $V_{1/2}$:-73.1mV, k:7.0mV in 3mM $[Ca]_o$, 2mM $[Na]_o$; means of 5 cells), and has a 1.7 to 2.6 fold slower inactivation time constant at -30 to -50mV than the classical I_{Na}. That I_{Ca}(TTX) channels activate over more negative potentials suggests they may be critical for depolarizing the membrane potential to action potential threshold and hence may have relevance for cardiac arrhythmias.

Tu-AM-B7

IONIC MECHANISMS OF PROPAGATION IN CARDIAC TISSUE: ROLES OF SODIUM AND L-TYPE CALCIUM CURRENTS DURING REDUCED EXCITABILITY AND DECREASED GAP-JUNCTION COUPLING. ((**Y. Rudy**, R.M. Shaw)) Cardiac Bioelectricity Research and Training Center, Case Western Reserve University, Cleveland, OH 44106-7207.

Reduced membrane excitability and reduced intercellular coupling both slow conduction velocity. Yet the mechanisms of slowed conduction for the two conditions are very different. We explored the ionic mechanisms of conduction slowing for both conditions using a multicellular theoretical fiber. The model consisted of ventricular cells (Luo-Rudy formulation) connected by gap-junctions. A safety factor of conduction was formulated, and computed for each condition.

Concomitant with conduction slowing, safety factor decreased with reduced excitability but increased with reduced intercellular coupling. These opposite effects on propagation safety were reflected in the minimum obtainable conduction velocity before failure: decreased excitability reduced velocity to only 1/3 of control before block occurred whereas decreased coupling reduced conduction velocity as much as 1/20 of control. For reduced excitability, the L-type calcium current, $I_{Ca(L)}$, did not aid conduction. However, $I_{Ca(L)}$ was a major influence to sustain conduction when intercellular coupling was reduced. Conduction failure occurred at 1/3 the intercellular conductance in the presence of normal $I_{Ca(L)}$. High intracellular calcium concentration, $[Ca]_i$, lowered propagation safety and caused earlier block when intercellular coupling was reduced. $[Ca]_i$ affected conduction via calcium-dependent inactivation of $I_{Ca(L)}$.

The increase of safety factor during reduced coupling suggests a major involvement of uncoupling in stable slow conduction in infarcted myocardium, making microreentry possible. Reliance on $I_{Ca(L)}$ for this type of conduction suggests $I_{Ca(L)}$ as a possible target for antiarrhythmic drug therapy.

Tu-AM-B8

MECHANISM OF ANODAL STIMULATION IN CARDIAC VENTRICULAR MYOCYTES ((**Ravi Ranjan**, Nipavan Chiamvimonvat, Gordon F Tomaselli, Eduardo Marban)) Johns Hopkins University, Baltimore, MD 21205

Anodal stimulation is routinely observed in cardiac tissue, but only recently has an explicit mechanism been proposed. All the current explanations use the results of bidomain cardiac tissue modeling and suggest that a virtual cathode induced in the tissue distant from the electrode is the site of initiation of depolarization. We considered the alternative possibility that the active membrane properties underlie anodal stimulation. In agreement with this idea, we find anode break excitation leads to action potentials in single cardiac ventricular myocytes from rabbit, guinea pig and dog. The basis of this cellular anodal excitation is the activation of a hyperpolarization-dependent inward current reminiscent of I_f. Upon release of the hyperpolarization, persistent inward "tail" current drives the transmembrane potential towards the activation threshold of the sodium current, initiating an action potential. The threshold of excitation of this current is ~ -200 mV in guinea-pig cells. Cellular anodal excitation can be simulated by a modified Luo-Rudy model which includes monovalent cation block of the inward rectifier and addition of the hyperpolarization activated, I_f-like current. This work is the first to document the existence of anode break responses in single heart cells. Active membrane properties recruited by hyperpolarization may form the basis of anodal stimulation in cardiac tissue.

Tu-AM-C1

CA/CALMODULIN-DEPENDENT PROTEIN KINASE II (CAMKII) STIMULATES UNITARY T-TYPE CA CHANNEL CURRENTS. ((H-K. Lu[1], J.J. Pancrazio[2], **P.Q. Barrett**[1])) Depts. [1]Pharmacology and [2]Anesthesiology, Univ. Virginia, Charlottesvile, VA. (Spon. by P.Q. Barrett)

In adrenal glomerulosa (AG) cells, T-type Ca channels link small changes in V_m to Ca-dependent hormone secretion. Activation of CaMKII amplifies this transduction by inducing a hyperpolarizing shift in the voltage-dependence of channel activation (Lu , AJP 1994). We examined the mechanisms underlying this change in gating behavior. We used the cell-attached patch-clamp technique to measure unitary currents in freshly isolated calf (3-7 days) AG cells. Consecutive depolarizations from -90 mV to -35 mV evoke small amplitude openings (0.57 pA) that inactivate slowly at -35 mV and show a slope conductance of 9.2 pS in 110 $BaCl_2$. In the presence of 140 mM K, raising bath Ca from 150 nM to 1 μM increases NPo 4-fold [1.4 ± 0.3% to 5.9 ± 0.9% (n= 10); p<0.01]. With Ca-stimulation, channel openings increase from 1400 to 5185 openings/1000 sweeps but open duration time constants [$\tau_{o,1}$= 0.3 msec, $\tau_{o,2}$= 2.3 msec, r= 0.98] remain unchanged. Preincubation with KN 62, a CaMKII inhibitor that competes with CaM for its binding site on the kinase, abolishes stimulation by 1 μM Ca [2.1 ± 0.2% to 2.6 ± 0.5% (n= 7); n.s]; stimulation is preserved with the inactive isomer, KN 04 [2.0 ± 0.8% to 6.2 ± 1.5% (n = 8); p<0.01]. In the excised-patch, channel activity persists at 50 nM Ca with 2.5 mM ATP, 500 μM GTP and 0.2 μM CaM. With 500 nM Ca, NPo increases 4-fold [0.8 ± 0.2% to 3.0 ± 0.9% (n= 8); p<0.05] and is inhibited by AIP, an autoinhibitory peptide of CaMKII [0.8 ± 0.2% to 0.9 ± 0.2% (n= 11); n.s.]. Preactivated CaMKII, ^{286}Asp-CaMKII, raises NPo in the absence of Ca elevation [0.5 ± 0.2% to 1.4 ± 0.2% (n= 9); p<0.01]. We conclude that CaMKII amplifies signaling by increasing the frequency of channel opening and that no other Ca-dependent effector is required to induce this change in gating.

Tu-AM-C2

INHIBITION OF EXPRESSED L-TYPE CALCIUM CURRENT BY NITRIC OXIDE DONORS. ((**Hai Hu** and Eduardo Marban)). The Johns Hopkins University School of Medicine, Baltimore, MD.

Nitric oxide donors have been reported to have complex effects on calcium current in native heart cells, with direct stimulation and indirect cyclic-GMP-mediated inhibition. To investigate the basis of these effects, we expressed various subunit combinations of cardiac and skeletal muscle L-type calcium channels in HEK 293 cells and exposed the cells to the NO donors SNAP (100-800 μM) or S-nitrosocysteine (100 μM - 1 mM). The currents were studied using whole-cell patch recordings with 2 -10 mM barium as the charge carrier. SNAP reduced the amplitude of calcium currents, with 75% inhibition of peak current through α_{1C}-β_{1a}-α_2 channels by 800 μM SNAP (n=5). A similar effect was observed in α_{1C}-β_{2a} channels. Co-expression of α_2 did not alter the response. S-nitrosocysteine also inhibited the calcium current. Considering all subunit permutations, NO donors never enhanced the current. The inhibitory effect of SNAP was not blocked by methylene blue (5 - 30 μM) or 8-Br-cyclic GMP (100 - 400 μM). We conclude that NO inhibits L-type calcium channels by a mechanism independent of cyclic-GMP. The effects reported in native heart cells cannot be reproduced in a mammalian expression system.

(α_{1C}: rabbit cardiac muscle; β_{1a}: rabbit skeletal muscle; β_{2a}: rat cardiac muscle; α_2: rabbit skeletal muscle.)

Tu-AM-C3

INHIBITION OF ISOPROTERENOL STIMULATION OF THE L-TYPE Ca^{2+} CURRENT IN GUINEA PIG VENTRICULAR MYOCYTES BY ENDOTHELIN-1: STUDIES INTO MECHANISMS

((**G.P. Thomas***, S.M. Sims[+] and M. Karmazyn*)) Depts. of Pharmacology and Toxicology* and Physiology[+],University of Western Ontario, London, Ontario, Canada.

Endothelin-1 (ET-1) has been shown to modulate cardiac function through various ion-regulatory processes. The present study examined the effect of ET-1 on basal and isoproterenol (ISO)-enhanced L-type Ca^{2+}current ($I_{Ca,L}$) in guinea pig ventricular myocytes. $I_{Ca,L}$ was recorded under nystatin perforated patch configuration which maintains physiological intracellular milieu. ET-1 at concentrations of 1, 5 and 10 nM had little effect on basal $I_{Ca,L}$. However, $I_{Ca,L}$ enhanced by ISO (500 nM) was significantly attenuated by 5 nM ET-1 by more than 50% compared to ISO alone. This suppression was reversed upon withdrawal of ET-1. $I_{Ca,L}$ enhanced by forskolin was only marginally decreased by ET-1. The inhibitory effect of ET-1 against ISO was completely blocked by the ET_A receptor antagonist BQ-123 (1μM). In ventricular myocytes incubated with pertussis toxin (PTX, 2 μg/ml) for 5 hours, ET-1 did not inhibit ISO-enhanced $I_{Ca,L}$. Although ET-1 has been shown to activate specific protein kinase C (PKC) isoforms, the PKC inhibitor bisindolylmaleimide (20 nM) failed to alter the effect of ET-1. We also studied potential interaction with nitric oxide (NO), however the NO donor SIN-1, (10 μM)) did not alter the ET-1 effect. Our results demonstrate a potent inhibitory effect of ET-1 against ISO-enhanced $I_{Ca,L}$ in the absence of any direct effect of the peptide. We demonstrate further that these effects are mediated by ET_A receptors coupled to PTX sensitive G-proteins although they are independent of PKC and unaffected by NO generation. ET-1 may be an important modulator of conditions associated with increased levels of catecholamines. (Supported by the Heart & Stroke Foundation of Ontario).

Tu-AM-C4

KINETIC COMPONENTS OF THE GATING CURRENTS OF HUMAN CARDIAC L-TYPE CA^{2+} CHANNELS ((**I.R. Josephson**)) Mol & Cell Physiol, Univ of Cincinnati, Cincinnati, OH.

The present work identifies the kinetic properties of human cardiac L-type Ca channel gating currents (Ig), and determines the relationship of these components to the activation of the Ca channel ionic current (ICa). Cloned human cardiac L-type Ca channel α_1+α_2+β_3 subunits were transiently expressed in HEK293 cells and Ca channel gating currents were recorded following the addition of 5 mM Co^{2+}. The kinetic components of the ON and OFF gating currents were identified using exponential curve fitting. Reconstruction of the two kinetic components of charge (QONfast and QONslow) yielded distributions that were similar in their voltage dependence and relative proportion to those measured directly by steady-state integration of QON1 and QON2. The time constants of the ON gating current decays were also present in the activation of ICa. The results suggest that: 1.) the activation of the human cardiac L-type calcium channel involves the movements of at least two, functionally distinct gating structures; 2.) a fast charge movement (~1/4 of the total charge; QON1 or QONfast) precedes a slower charge movement (~3/4 of the total charge; QON2 or QONslow) and 3.) channel opening is associated with the conformational change(s) producing QONslow.

Tu-AM-C5

DUAL CONTROL OF THE MUSCARINIC INHIBITION OF $I_{Ca,V}$ BY p38 AND ERK MAPK PATHWAYS IN INSULINOMA (INS-1) CELLS. ((**M.A. Wilk-Blaszczak**, K. Shih, M. Cobb, and F. Belardetti)) Dept. Pharm., U.T. Southwestern, Dallas, TX 75235.

We have previously shown that the p38 mitogen-activated protein kinase (MAPK) pathway mediates inhibition of $I_{Ca,V}$ by bradykinin in neuroblastoma-glioma (NG108-15) cells (Wilk-Blaszczak and Belardetti, Soc. Neurosci. Abs., 1996). The $I_{Ca,V}$ couples glucose-induced depolarization to insulin secretion in pancreatic β cells. We have used the insulin-secreting insulinoma cell line INS-1 and investigated the role of MAPK pathways in the modulation of $I_{Ca,V}$ by muscarinic receptors. We have now found that at stimulatory concentrations of glucose (10 mM), muscarinic agonists produced a robust inhibition of $I_{Ca,V}$ (20-30%). This inhibitory effect was blocked by intracellular dialysis with SB203580, an inhibitor of the p38 MAPK (10 μM; n=11), but not by SKF106978, an inactive analog (10 μM; n=10). We also found that substimulatory concentrations of glucose (3 mM) or incubation of the cells with PD98059 (an inhibitor of MEK, which in turn activates ERK; 10 μM, n=12) in 10 mM glucose attenuated the muscarinic response (to 5-10%). The DMSO vehicle (n=9), or PD98059 in 3 mM glucose (n=11) were without effect. Thus the p38 MAPK pathway is likely to mediate muscarinic inhibition of $I_{Ca,V}$ in INS-1 cells. In addition, together with the evidence that high glucose stimulates ERK (Shih and Cobb, submitted), these observations suggest that inhibition of $I_{Ca,V}$ by muscarinic receptors is facilitated by glucose via the ERK MAPK pathway.

Tu-AM-C6

PROPERTIES OF DIHYDROPYRIDINE-SENSITIVE SINGLE Ca^{2+} CHANNELS IN THE SOMA AND AXONS OF *HERMISSENDA* PHOTORECEPTORS. ((**[1]E. N. Yamoah** & [2]L. D. Matzel)) [1]Johns Hopkins School of Medicine, Dept. of Physiology, Baltimore, MD 21205. [2]Rutgers University, Dept. of Psychology, Busch Campus, New Brunswick, NJ, 08903.

Previous studies in *Hermissenda* type B photoreceptors have indicated that Ca^{2+} influx through voltage-gated channels in the axons and soma during depolarization, associated with classical conditioning, initiates changes in the intrinsic membrane properties of the B cells. We examined whole-cell Ca^{2+} currents in the soma of the B cells and single-channel Ca^{2+} currents at different segments of the B cell axons. Two distinct Ca^{2+}channels were recorded in the soma; DHP-sensitive (L-type) and DHP-insensitive (T-type) channels. At the axons, we report the presence of a DHP-sensitive channel with a small conductance (γ=8-12 pS; see Fig. 1) which is uncharacteristic of the traditional L-type Ca^{2+} channels (γ > 20 pS). At a step potential of -20 mV, two time constants were estimated for the open ($\tau_{open,1}$ ~ 0.09 and $\tau_{open,2}$ ~ 2 ms) and close ($\tau_{close,1}$ = 0.17 ms and $\tau_{close,2}$ 4 ms) times of the channel. Axonal Ca^{2+} channels were unevenly expressed along the length of the axon with higher density of expression occurring at the lateral one-third, close to the terminal branches.

Fig. 1

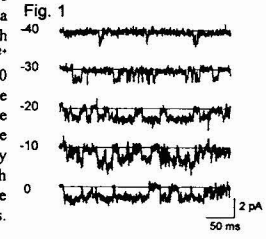

Tu-AM-C7

BARIUM-DEPENDENT INACTIVATION OF L-TYPE CALCIUM CHANNELS. ((**G. Ferreira**, J. Yi, E. Ríos and R. Shirokov)) Rush University, Chicago, IL 60612.

Inward Ba^{2+}currents (I_{Ba}) were recorded in tsA201 cells transfected with cDNA of Ca^{2+} channel subunits α_{1C} and β_{2a}. During a 20 s pulse, I_{Ba} decayed as the sum of two exponential functions, each accounting for about half of the decay at 20 mV, with time constants τ_{fast} = 0.6 ± 0.05 s and τ_{slow} = 6.7 ± 0.8 s. τ_{slow} monotonically decreased with voltage, whereas τ_{fast} was slightly increased at high voltages. Whereas the amplitude of the slow phase increased at high voltages, the amplitude of the fast phase decreased resulting in a "U-shape" that mirrors the voltage dependence of current amplitude. The amount of gating intramembrane charge declined as a single exponential, with time constant similar to τ_{slow} (8.7 ± 1 s at 20 mV). Therefore, the fast decay of I_{Ba} had no gating charge correlate. The rate of recovery of I_{Ba} also had a non-monotonic dependence on conditioning voltage, being slower at 20 mV than at 60 mV. Ba^{2+} entry during long pulses did not change the current's reversal potential, indicating that neither decay phase was due to a change in driving force. With Na^+ as charge carrier, the current decreased as a single exponential with time constant similar to τ_{slow}. The results are evidence that the slow phase in I_{Ba} decay reflects voltage-dependent inactivation, while the fast phase is caused by a Ba^{2+}-dependent mechanism. Because the fast phase was present in native rabbit ventricle myocytes and cells expressing different combinations of α_{1C}, β_{2a} and $\alpha_2\delta$, it must be a property of α_{1C}.

Simulations with the inactivation model of Shirokov et al. (*J.Gen.Physiol.* 102, 1993) reproduced the observations assuming a weak binding of Ba^{2+} to the α_1 site that controls Ca^{2+}-dependent inactivation. Supported by NIH and AHA-MC.

Tu-AM-C8

EFFECT OF THE $\alpha_2\delta$ SUBUNIT ON VOLTAGE-DEPENDENT INACTIVATION OF CARDIAC Ca^{2+} CHANNELS. ((**R. Shirokov**, G. Ferreira, J. Yi, and E. Ríos)). Rush University, Chicago, IL 60612.

Ba^{2+} currents (I_{Ba}) and gating currents of Ca^{2+} channels were recorded in tsA201 cells transiently transfected with $\alpha_{1C}+\beta_{2a}$ and $\alpha_{1C}+\beta_{2a}+\alpha_2\delta$ cDNAs. With both subunit combinations I_{Ba} decayed bi-exponentially (in $\alpha_1+\beta$, τ_{slow} = 6.7±0.8 s and τ_{fast} = 0.6±0.05s at 20mV) . $\alpha_2\delta$ made the slow decay of I_{Ba} more rapid (τ_{slow} = 3.9±0.4 s) but did not change τ_{fast}. As shown by Ferreira *et al.* (this meeting), at 20 mV the availability of gating charge mobile at positive potentials (charge 1) decreased slowly, in parallel with the slow component of I_{Ba} decay (τ =8.7±1 s with $\alpha_1+\beta$). This reduction occurred more rapidly with $\alpha_2\delta$ (4.5±2.7 s). As demonstrated previously with native channels, together with reduction of charge 1 a fraction of charge became mobile between -60 and -150 mV (charge 2). After a 5s pulse, charge 2 was 33 ± 4% of the total in $\alpha_1+\beta$ and 56 ± 5% with $\alpha_2\delta$. Neither the kinetics of charge 2 at -150 mV, nor those of recovery of charge 1 (τ≈120 ms at -60 mV) were affected by the $\alpha_2\delta$ subunit.

As shown in work on Na^+ channels, cardiac Ca^{2+}channels and skeletal muscle DHP receptors, the appearance of charge 2 upon channel inactivation reflects the different voltage dependence of transitions among inactivated states, and is consistent with an intrinsically voltage-independent inactivation step. Because $\alpha_2\delta$ hastened the decay of I_{Ba} and available charge, and increased charge 2, but spared its kinetics and the kinetics of recovery, the subunit must work by accelerating the inactivating transition, without influencing the movement of voltage sensors. Supported by NIH and AHA-MC.

Tu-AM-C9

SINGLE CHANNEL PROPERTIES OF TYPE-2 AND TYPE-1 INOSITOL 1,4,5-TRIPHOSPHATE RECEPTOR ((**J. Ramos-Franco***, G.A. Mignery and M. Fill)), *Instituto Nacional de Cardiología, Mexico City, México, and Loyola University Chicago, Maywood. IL 60153.

Molecular cloning has revealed the existence of different $InsP_3Rs$ in a variety of cell types. Multiple receptor isoforms implies that the different $InsP_3Rs$ may be functionally heterogeneous. Populations of type-1 $InsP_3Rs$ were isolated from cerebellum. Populations of type-2 $InsP_3Rs$ were isolated from acutely dissociated ventricular cardiac myocytes. Single channel properties of both the type-1 and type-2 channels were defined in planar lipid bilayers (PE/PC, 7:3; 50 mg/ml decane). Recording solutions contained 220 mM $CsCH_3SO_3$ cis (20 mM trans), 10 mM HEPES (pH 7.4) and 1 mM EGTA (200 nM $[Ca^{2+}]_{free}$). The type-1 and type-2 $InsP_3R$ channels were both characterized by multiple conduction states, slow & fast open events, and similar Ca^{2+} selectivity. Both channels have similar permeation properties with a main conductance of 388 pS with Cs^+ as charge carrier 100 pS with Ca^{2+} as charge carrier. Infrequent spontaneous single channel events were observed in the absence of added $InsP_3$. $InsP_3$ (cytoplasmic side) activated both type-1 and type-2 channels with half-maximal open probability occurring at 58 nM for type-2 and 173 nM for type-1. This is consistent with the difference between the type-1 and type-2 $InsP_3$ binding affinities reported previously (Sõdhof et al., 1991). The Hill coefficient of the $InsP_3$ activation curves were 0.77 and 1.85 for the type-1 and type-2 channels, respectively. At saturating $InsP_3$ concentrations, the maximal Po was 0.55 for type-2 and 0.20 for type-1. Both the type-1 and type-2 channels were heparin sensitive and were not blocked by ryanodine (7 μM). Thus, these data indicate that the type-1 and type-2 $InsP_3R$ channels have similar permeation properties but differ in their $InsP_3$ sensitivity. It appears that $InsP_3$ affinity, cooperativity and efficacy of the $InsP_3$ activation process are type specific.
Supported by AHA (GAM & MF) NIH MH53367 (GAM) and NIH NS-29640 (MF).

REGULATION OF ION CHANNELS: ANION CHANNELS

Tu-AM-D1

VOLUME-SENSITIVE ANION CHANNELS IN MICROGLIA AND LYMPHOCYTES: CONSERVED BIOPHYSICS BUT DIFFERENT REGULATION. ((**L.C. Schlichter**, M.C. Chang, G. Sakellaropoulos)) Univ. of Toronto, Dept. of Physiology and Playfair Neuroscience Unit.

Volume-sensitive anion (Cl^-) channels are found in many cells; their properties and pharmacology vary considerably. Many are apparently small-conductance (< 2 pS) channels from stationary noise analysis. Recently, Jackson and Strange (J.Gen. Physiol., Vol.105, 1995) raised the possibility that the channels are much larger (15-50 pS), being always open once activated, possibly by membrane insertion after cell swelling. We have used non-swelling and swelling conditions to study further the biophysical properties of volume-sensitive Cl^- channels in two types of immune cell: human T lymphocytes (both resting and activated cells) and in microglia, the brain's resident immune cell. We exploited the weakly voltage-dependent block of these channels by DIDS to reduce their probability of opening. We have shown that DIDS decreased outward current by reducing Cl^- current only, not by activating another current. Under all conditions tested, single-channel conductance was of the order of 1 pS, even at very positive potentials. We further compared the properties of the microglia and lymphocyte anion channels. Despite similarities in anion selectivity, voltage independence of gating, and pharmacology, the channels in the two cell types differed in their dependence on ionic strength, nucleotide requirements and volume-sensitivity. Internal pipette-perfusion studies of microglia showed an absolute requirement for cytoplasmic nucleoside triphosphates, but nucleotide hydrolysis was apparently not necessary to activate the current. We conclude that the biophysical properties are conserved, whereas channel regulation is cell-type specific. (Supported by NSERC, MRC Canada)

Tu-AM-D2

A POTASSIUM-ACTIVATED CHLORIDE CONDUCTANCE: A GENERAL ROLE IN VOLUME REGULATION? ((M. Steinert and S. Grissmer)). Department of Applied Physiology, University of Ulm, 89081 Ulm, Germany.

The whole-cell recording mode of the patch-clamp technique was used to study the effect of extracellular K^+ and Rb^+ on membrane currents in human osteoblasts, a human osteoblast-like cell line, and in the Jurkat human leukaemic T cell line. Increasing $[K^+]_o$ from 4.5 to 160 mM increased the membrane conductance of all the different cells 10-100 -fold. This increase of membrane conductance was due to the activation of a Cl^- conductance as judged from reversal potential measurements. Rb^+ was also able to induce this conductance, however, conductance was less than half in Rb^+ compared to K^+. The K^+-induced Cl^- conductance showed no voltage- or time-dependent gating behavior at potentials between -80 and +80 mV. DIDS and SITS blocked the K^+-induced Cl^- current in a voltage-dependent manner, the degree of blockade increasing with membrane depolarization. The permeability sequence of the induced anion conductance was $I^- > Cl^- \geq NO_3^- >$ aspartate. The activation of the Cl^- conductance by K^+ could be inhibited by hypertonic solutions. In addition, the activation of a Cl^- conductance by hypotonic solutions could be enhanced by extracellular K^+. We conclude that an outwardly rectifying Cl^- conductance can be activated either upon osmotic swelling or by an increase in extracellular K^+. Both activation pathways may be involved in cell volume regulation and seem to apply to volume-sensitive Cl^- channels in general since we observe this phenomenon in different cell types. The K^+-dependence of the Cl^- conductance provides a mean for the regulation of Cl^- efflux when K^+ accumulates in the extracellular medium either through K^+ loss from the same cell or cells in the vicinity. The unusual dependence of this Cl^- conductance on the extracellular monovalent cation concentration may be a mechanism whereby cells under either osmotic stress or an increase in $[K^+]_o$ could control Cl^- flux thereby fine tuning regulatory volume decrease. The results also suggest the presence of an external potassium binding site on the Cl^- channels that may act as a modulator/activator for this anion conductance. Supported by grants from Pfizer Inc, DFG (Gr848/4-1), Pfizer Ltd, and the BMBF (IZKF Ulm, B4).

Tu-AM-D3

MULTIFUNCTIONAL CALCIUM/CALMODULIN DEPENDENT PROTEIN KINASES MEDIATE INACTIVATION OF Ca^{2+}-ACTIVATED Cl CHANNELS IN AIRWAY MYOCYTES ((**Y.-X. Wang** and M. I. Kotlikoff)). Department of Animal Biology, University of Pennsylvania, 3800 Spruce Street, Philadelphia, PA 19104-6046. (Spon. by Y.-X. Wang)

Ca^{2+}-activated chloride currents ($I_{Cl(Ca)}$) may play a role in excitation-contraction coupling in smooth muscle. In this study, membrane currents and intracellular Ca^{2+} concentration ($[Ca^{2+}]_i$) were simultaneously measured in Fura-2 loaded, equine tracheal myocytes to determine the cellular mechanism for inactivation of $I_{Cl(Ca)}$. In cells recorded using the nystatin method, $I_{Cl(Ca)}$ rapidly inactivated (V_H=-60 mV) even though a sustained increase in $[Ca^{++}]$ was achieved using ionomycin. Conversely, the calcium-activated potassium current was sustained under these conditions. Intracellular dialysis of 1 mM ADP or AMP-PNP significantly delayed the inactivation of $I_{Cl(Ca)}$ induced by ionomycin, although the $[Ca^{2+}]_i$ increase was not affected. Following intracellular dialysis of either the calmodulin antagonist W7 (50 μM), or the inhibitor of multifunctional calcium/calmodulin dependent protein kinase KN93 (50 μM), the inactivation of $I_{Cl(Ca)}$ induced by ionomycin was delayed, and the increase in $[Ca^{2+}]_i$ was not different than control. Intracellular dialysis of the non-selective kinase inhibitor H7 (60 μM, predicted to block 91% of c-GMP-dependent protein kinase, 95% of c-AMP-dependent protein kinase, and 91% of protein kinase C) did not produce an appreciable effect on the sustained $[Ca^{2+}]_i$ increase or the inactivation of $I_{Cl(Ca)}$. We conclude that the inactivation of $I_{Cl(Ca)}$ is mediated by protein phosphorylation, and that the signaling pathway may involve CaM kinase II.

Tu-AM-D4

FAST ACTIVATION OF CFTR CHLORIDE CHANNELS, INCORPORATED INTO A BLM, BY AN ATP CONCENTRATION JUMP. ((G. Nagel, A. Wellan-Ely, E. Bamberg, T. Jensen*, J.R. Riordan*)) MPI für Biophysik, D-60596 Frankfurt, F.R.G. & *Mayo Clinic Scottsdale, AZ, U.S.A.

The influence of fast ATP concentration changes on gating of CFTR was investigated using flash photolysis of caged ATP, a non-hydrolyzable ATP derivative. Plasma membrane vesicles from BHK (or CHO, or HEK 293) cells expressing CFTR were incorporated into black lipid membranes (BLM). After verification of CFTR incorporation by the appearance of chloride selective channels (about 7 pS conductance at 300 mM Cl^-) in the presence of ATP and PKA cat. subunit, the ATP concentration was lowered by the addition of hexokinase and glucose which led to the closing of the CFTR channels. Addition of caged ATP did not open channels, but a short u.v. light flash resulted in a fast opening of CFTR channels that could be fitted by a monoexponential function with a time constant of about 2 s at 22°C. Caged ATP in the presence of ATP weakly reduced the open probability of CFTR channels. Single channel experiments revealed two closed times, the slower one being very similar to the time constant obtained from photolysis experiments. UV flash experiments at 29°C, indicating a high activation energy of the time constant, support the hypothesis that ATP hydrolysis is involved in CFTR channel opening.
(Supported by MPG, DFG, NIH, and CF Foundation.)

Tu-AM-D5

MODIFICATION OF CYSTEINE RESIDUES MODULATES GATING OF THE CYSTIC FIBROSIS Cl- CHANNEL. ((**Melissa A. Harrington**, Kevin, L. Gunderson, Ron R. Kopito)) Department of Biology, Stanford University, Stanford, CA 94305.

The cystic fibrosis transmembrane conductance regulator (CFTR) is a chloride channel with complex regulation. Channel gating requires both hydrolysis of ATP and phosphorylation by PKA. In both cell-free and cell-attached patches, the reducing agents B-mercaptoethanol (B-ME) and dithiothreitol (DTT) increase the activity of CFTR stably expressed in HEK-293 cells. When added to forskolin-activated cells, B-ME significantly increases the open probability and average current through CFTR channels in cell-attached patches. Similarly, B-ME significantly increases the open probability and average current of CFTR channels measured in inside-out patches even in the absence of kinases. The effect of reducing agents on CFTR channel activity is quite complex. BME and DTT increase both the opening and closing rates of the channel, thereby increasing the number of openings while shortening the mean open time. This combination of effects could be explained if reducing agents increased the ATP hydrolysis rate at both nucleotide binding domains (NBFs). Faster hydrolysis at NBF2 would promote faster closing, while increasing NBF1 hydrolysis could cause the channel to open more frequently. This hypothesis is supported by the fact that under oxidizing conditions, channels show the "locked open" gating seen in the presence of non-hydrolyzable nucleotides. It is likely that these effects are mediated by modification of cysteine residues in the protein as prior exposure to NEM blocks the effect of reducing agents.

Tu-AM-D6

THE R DOMAIN IS REQUIRED FOR THE NORMAL FUNCTION OF CFTR CHLORIDE CHANNEL. ((**Jianjie Ma**, Mitchell L. Drumm*, Jiying Zhao, Junxia Xie, Jianxun Yi, and Pamela B. Davis)). Dept. of Physiology & Biophys., & Pediatrics*, Case Western Reserve Univ. (Spon. by D. Dearborn)

cAMP-dependent phosphorylation of serine residues in the regulatory (R) domain is a pre-requisite for opening of the CFTR chloride channel. To understand the molecular mechanism of R domain regulation of the CFTR channel, two mutant forms of human epithelial CFTR were constructed: three conserved proline residues (a.a. 740, 750 and 759) were mutated to alanines (**R-P3A**), and 128 amino acids were removed from the R domain (**ΔR(708-835)**). R-P3A formed a PKA- and ATP-regulated chloride channel, with open probability approximately 2-fold higher than the wild type CFTR channel (Po=0.318±0.022, wt-CFTR; 0.652±0.043, R-P3A). ΔR(708-835) formed a constitutively open chloride channel independent of PKA phosphorylation, with open probability significantly less than that of the wt-CFTR channel (Po=0.122±0.012, ΔR(708-835)). The reduced activity of the ΔR(708-835) channel was due at least in part to the altered function of the nucleotide-binding folds, for compounds such as AMP-PNP and pyrophosphate which increased the open lifetimes of the wt-CFTR channel had no effect on the ΔR-CFTR channel. Vanadate, which enhanced the function of the wt-CFTR channel, instead inhibited the activity of the ΔR(708-835) channel. Our data suggest that proper conformation of the R domain is essential for the normal function of the CFTR channel. Supported by NIH and CFF.

Tu-AM-D7

DEFECTIVE PHOSPHORYLATION ACTIVATION OF THE ΔF508 CFTR. ((T. -C. **Hwang** and L. Al-Nakkash)). Department of Physiology, Dalton Cardiovascular Research Center, University of Missouri-Columbia, Columbia, MO 65211.

Deletion of phenylalanine 508 (ΔF508) accounts for ~70% of disease-associated mutations in cystic fibrosis. In cell-free systems, the Po of wild-type (wt) and ΔF508-CFTR are not different (Li, C. et al., *Nature Genetics* 3:311-316). However, in cell-attached patches, the Po for ΔF508-CFTR is only ~17% of that for wt-CFTR under maximal cAMP stimulation (10 μM forskolin or 200 μM CPT-cAMP). While the open times of ΔF508-CFTR are not significantly different from those of wt-CFTR, one of the closed time constants is different by one order of magnitude (estimated $\tau_{c(\Delta F508)}$ > 30 s and $\tau_{c(wt)}$ of ~3 s). This difference in forskolin-induced channel activity between wt- and ΔF508-CFTR is not due to differences in cytosolic regulatory mechanisms because wt-CFTR, when "transplanted" to cells expressing ΔF508-CFTR using the patch-cramming technique, showed active response to forskolin stimulation as in the native cells. Since $\tau_{c(wt)}$, a time constant not seen in cell-free systems, was drastically increased to >25 s by reducing [forskolin] to 50 nM (or using low [CPT-cAMP]), it likely reflects the phosphorylation activation step of CFTR. Genistein, a tyrosine kinase inhibitor, increased forskolin-activated wt- and ΔF508-CFTR currents by 3 and 19 fold respectively through an increase in the open times and a decrease in the closed times. Mean current-variance analysis of macroscopic currents demonstrated that the Po for wt- and ΔF508-CFTR are identical in the presence of forskolin and genistein, suggesting that genistein completely restores ΔF508 channel activity. Thus, deletion of phenylalanine 508, an amino acid in the first nucleotide binding domain (NBD1), causes defects in the phosphorylation activation process that occurs at the regulatory (R) domain. These results suggest a structural/functional coupling between the NBD and R domains. Supported by the NIH, the CF Foundation, and the Research Board, University of Missouri.

Tu-AM-D8

EFFECTS OF GENISTEIN ON CFTR CHLORIDE CHANNEL GATING ((**Fei Wang** and Tzyh-Chang Hwang)) Department of Physiology, Dalton Cardiovascular Research Center, University of Missouri, Columbia, MO 65211. (Sponsored by V. Huxley)

Genistein increased CFTR channel activity in the presence of a maximally effective concentration of forskolin (10 μM) in cell-attached patches. Part of this potentiation effect is through prolongation of the channel open time (Yang, I. et a., *Am. J. Physiol.*, 1996, in press). Since genistein competitively inhibits ATP binding to tyrosine kinases, we test the hypothesis that genistein affects CFTR gating through binding to CFTR. Wild-type human epithelial CFTR channels were recorded in excised inside-out patches from Hi-5 insect cells infected with baculovirus containing CFTR cDNA. CFTR channels were first activated by forskolin (10 μM) plus calyculin A (50 nM), a membrane-permeant phosphatase inhibitor, in cell-attached patches; membrane patches were then excised into an inside-out configuration. Gating of CFTR chloride channels was examined by pulse application of ATP (0.5 mM) with or without genistein. Genistein (25 μM) did not open phosphorylated CFTR channels by itself, but increased the ATP-induced CFTR channel current by 2.18 ± 0.74 fold (n = 11). A similar magnitude of enhancement was observed when genistein was applied with PKI (3 μM, a specific PKA inhibitor) or VO_4 (10 μM, a non-specific tyrosine phosphatase inhibitor). Thus, it is unlikely that inhibition of protein phosphatases or tyrosine kinases can account for genistein's effects. The potentiation effect increases with increasing concentrations of genistein and reaches a maximum of 3.31 ± 1.86 fold (n = 10) at 35 μM of genistein. In the absence of genistein, both open time and closed time histograms can be fitted with a single exponential function, yielding a mean open time (τ_o) of 0.302 ± 0.002 s and a mean closed time (τ_c) of 0.406 ± 0.003 s. In the presence of genistein, the open time histogram can be fitted with a double exponential function with τ_{o1} = 0.429 ± 0.003 s and τ_{o2} = 2.033 ± 0.173 s. Thus, genistein induces a prolonged open state, an effect that mimics that of nonhydrolyzable ATP analogs. However, when [genistein] is > 50 μM, a decrease of ATP-induced CFTR channel current was seen. Closed time histogram showed that genistein causes a prolonged closed state with a time constant of 2.410 ± 0.035 s. We thus conclude that 1) The effects of genistein are likely caused by a direct binding of genistein to the CFTR protein and 2) At least two binding sites are required to explain genistein effects: a high affinity site that decreases the closing rate and a low affinity site that reduces the opening rate.

Tu-AM-D9

XANTHINE DRUG ACTIVATION OF CFTR CHANNELS EXPRESSED IN HEK293 CELLS. ((**N. Arispe**, J. Ma and H. Pollard)) LCBG, NIDDK, NIH and Dept of Anatomy and Cell Biology, USUHS, Bethesda MD. 20814 and Dept. Physiol. and Biophysics, Case Western Reserve University, Cleveland, OH 44106

Microsomal membrane vesicles carrying the expressed CFTR protein were incorporated in planar lipid bilayers, and the resulting anionic currents were studied in the presence of N-phenylanthranilic acid (DPC), and the xanthine drug cyclopentyl-dipropylxanthine (CPX) and diallylcyclopentylxanthine (DAX). Two anionic conductances, *ca.* 10 and 2.5 pS, in a KCl gradient, were found associated with expression of CFTR. DPC affects both conductances by reducing the unitary current amplitude in a concentration and voltage dependent manner and by generating variable long periods of electrically silent activity. CPX and DAX robustly activate both anionic conductances increasing both frequency and duration of unitary events, achieving a maximum activation at concentration of 500 nM. Higher concentrations of CPX produce a decline in the open time probability of CFTR channels. However, higher concentrations of DAX produce maintained activation at saturation levels. We conclude that that the enhanced chloride efflux on CF cells produced by these xanthines analogues may be explained on the basis of the activation of CFTR channels.

VISUAL RECEPTORS

Tu-AM-E1

HOW DOES ONE RHODOPSIN MOLECULE TRIGGER A REPRODUCIBLE PHOTORESPONSE? ((**F. Rieke** and D. A. Baylor)) Dept. of Neurobiology, Stanford Medical School, Stanford, CA 94305.

The dark-adapted visual system can count photon absorptions with a reliability limited by dark noise in the rod transduction current and statistical fluctuations in the number of absorbed photons. Reliable photon counting requires the retinal rod to generate reproducible responses to absorbed photons. Since photoexcited rhodopsin catalytically activates a G-protein cascade, one might expect stochastic fluctuations in rhodopsin's catalytic lifetime to produce large fluctuations in the size and shape of the single photon response. Instead, each effectively-absorbed photon produces a nearly identical change in the rod's membrane current. We have investigated the mechanism of reproducibility in intact toad rods and truncated, internally-dialyzed rod outer segments. Our experiments indicate that local saturation of the electrical response or of intermediate steps in the amplifying cascade cannot explain reproducibility. Thus rhodopsin shutoff itself must follow a stereotyped time course. Tests indicate that reproducible rhodopsin shutoff is not produced by feedback control involving changes in internal calcium, activated transducin, or any of its downstream products. Measurements of rhodopsin's catalytic lifetime reveal a long time course not explained by known biochemical steps. We hypothesize that a series of intramolecular transitions allows photoexcited rhodopsin to shut off with a stereotyped time course.
Supported by National Eye Institute grants EY01543 and EY06456.

Tu-AM-E2

NMR STUDIES OF CALCIUM-BOUND RECOVERIN CONTAINING A POLAR MYRISTOYL ANALOG ((**J.B. Ames**[1], T. Tanaka[2], J.I. Gordon[3], M. Ikura[2], and L. Stryer[1])) Dept. of Neurobiology, Stanford Univ.[1]; Ontario Cancer Inst., Univ. of Toronto[2]; Dept. of Molecular Biology and Pharmacology, Washington Univ.[3]

Recoverin, a new member of the EF-hand superfamily, serves as a Ca^{2+} sensor in vision. A myristoyl or related N-acyl group covalently attached to the N-terminus of recoverin enables it to translocate to disc membranes when the Ca^{2+} level is elevated. Ca^{2+}-bound recoverin prolongs the lifetime of rhodopsin by blocking its phosphorylation. The NMR solution structure of Ca^{2+}-free recoverin shows that the myristoyl group is sequestered in a deep hydrophobic cavity (Tanaka et al.,*Nature* **376**, 444). The low solubility of Ca^{2+}-bound myristoylated recoverin has previously prevented determination of its structure. A polar analog of myristic acid (13-oxatetradecanoic acid) has been incorporated into recoverin to increase its solubility. 13-oxa recoverin binds two Ca^{2+} with a higher affinity (3 μM) than does native recoverin (17 μM) and exhibits Ca^{2+}-induced membrane binding. NMR spectra of 13-oxa recoverin are almost identical to spectra of native myristoylated recoverin. Complete sequence-specific NMR assignments have been obtained for 13-oxa recoverin and serve as a basis for determining its three-dimensional structure. The structure of Ca^{2+}-bound 13-oxa recoverin appears to be very similar to the x-ray crystal structure of $(Ca^{2+})_1$-unmyristoylated recoverin and to our recent NMR derived structure of $(Ca^{2+})_2$-unmyristoylated form. Four EF-hand motifs are arranged in a linear array, with Ca^{2+} bound to EF-2 and EF-3. The structure of the C-terminal domain is similar in Ca^{2+}-free and Ca^{2+}-bound recoverin, whereas their N-terminal domains are different. The most striking difference is that the amino-terminal myristoyl group is sequestered in the Ca^{2+}-free protein, whereas the amino-terminal region flips out into the solvent and becomes disordered in the Ca^{2+}-bound state. Biosynthetic incorporation of polar analogs of myristic acid may increase the solubility and make feasible the determination of structure of myristoylated proteins generally.

Tu-AM-E3

PHOTORECEPTOR RHODOPSIN: A STRUCTURAL AND CONFORMATIONAL STUDY OF 11–*cis* RETINAL IN RHODOPSIN IN ORIENTED MEMBRANES BY DEUTERIUM SOLID STATE NMR

((**G. Gröbner**[*], G. Choi[*], I. Burnett[*], P. Verdegem[#], J. Lugtenburg[#], C. Glaubitz[*] and A. Watts[*])) ([*]) Department of Biochemistry, Oxford University, Oxford, OX1 3QU, Great Britain, ([#]) Rijksuniversiteit de Leiden, NL–2300 RA Leiden, The Netherlands, (Spon. by I. Campbell)

Once excited by light, the membrane bound seven helix receptor rhodopsin initiates a G–protein second messenger amplification cascade mechanism, finally stimulating a nervous response. The first step in activating the rhodopsin is the photo–isomerization of its chromophore 11–*cis* retinal. The conformation and structure of the bound retinal are unknown due to the lack of precise (sub–nm) structural data for the protein. We are using a novel *ab initio* solid state ^2H NMR approach to study the conformation and orientation of deuterated retinal in unaxially oriented photoreceptor–containing membranes, using a new alignment technique; isopotential spin–dry ultracentrifugation. Phosphorous–31 NMR is used to monitor the integrity of the bilayers and to obtain the mosaic spread of the oriented sample. The orientational dependence of the ^2H NMR lineshapes with respect to the applied magnetic field has been analysed to give precise angles for each C–CD_3 bond vectors, finally leading to a accurate description of the retinal conformation.

Tu-AM-E4

AN ATOMIC MODEL OF TRANSMEMBRANE DOMAIN OF BOVINE RHODOPSIN FROM EXPERIMENTALLY DERIVED STRUCTURAL RESTRAINTS ((**P. Herzyk** and R.E. Hubbard)) Department of Chemistry, University of York, York, YO1 5DD, UK.

An atomic model of the transmembrane domain of bovine rhodopsin has been generated using a unique modelling procedure which builds a seven-helix bundle from experimental data. In the first stage, transmembrane helices are aggregated into a 3-D bundle by global optimisation of a penalty function built from the structural restraints extracted from the available experimental and theoretical data. The optimisation is achieved with a Monte Carlo Simulated Annealing technique using a simplified protein representation. In the second stage, the model is converted into the full-atom representation using the Molecular Dynamics Simulated Annealing technique. The structural restraints are derived from analysis of experimental information from biophysical studies on native and mutant proteins, from analysis of sequence of related proteins and from theoretical considerations of protein structure. In particular, relatively new data is used including: the 2-D projection map of frog rhodopsin, ^{13}C NMR data on Glu-113 counterion position with respect to retinal, steric complementarity of selected residues from helices C and F, relations between distances from Schiff base and mutated counterions at positions 90, 113 and 117, EPR data on the orientation of selected residues in helix C and D.

Tu-AM-E5

cGMP-GATED CHANNELS OF CONE PHOTORECEPTORS ARE MODULATED BY AN ENDOGENOUS CALCIUM BINDING MOLECULE PARTIALLY MIMICKED BY CALMODULIN. ((**David H. Hackos** and Juan I. Korenbrot)) Dept. of Physiology. University of California at San Francisco. San Francisco, CA 94143

We investigated the properties of cGMP-dependent currents in membrane patches detached from the outer segment of cone photoreceptors in fish. In patches detached in the presence of Ca^{++} (20 μM) and Mg^{++} (100 μM) the dependence of current amplitude on cGMP was well described by a Hill equation with $K_{1/2}$=99 uM and n=2.8. Exposure of these patches to EDTA (5 mM)/EGTA (5 mM) shifted the cGMP dependence to $K_{1/2}$=79 uM and n=1.9. Addition of 200nM calmodulin (CaM) with Ca^{++} (20 μM) and Mg^{++} (100 μM) to EDTA/EGTA-exposed patches shifted the cGMP dependence to $K_{1/2}$=88 and n=2.3, values near but significantly different from those measured before EDTA/EGTA exposure. The effect of CaM could be reversed repeatedly by exposure to EDTA and EGTA. However, CaM was ineffective in patches never exposed to EDTA and EGTA. Thus, the channels appear to be modulated by an endogenous molecule that is bound in the presence of Ca^{++} and Mg^{++} and is released in their absence. This molecule competes with CaM, but may not be identical to CaM.

In the presence of 200 nM CaM, the sensitivity of current amplitude to cGMP decreases with added Ca^{++}. This dependence is described by a Hill equation with $K_{1/2}$=340 nM and n=1.6. These numbers are different in the channels of tiger salamander rods, where $K_{1/2}$=680 and n=1.8. CaM concentration in intact rods is about 5 uM. Calculations suggest that at this concentration the $K_{1/2}$ of the Ca^{++} dependence would shift to about 25 nM, making a functional role for this Ca-dependence unlikely. In cones, the concentrations of CaM and the endogenous regulator are unknown. If the modulator in cones exists at concentrations lower than CaM in rods, then the $K_{1/2}$ of the Ca^{++} dependence may be within the physiological concentration range of cytoplasmic Ca^{++} in the intact cell and may, therefore, play a functional role.

Tu-AM-E6

Calcium fluxes in photoreceptors of *Drosophila* mutants lacking calmodulin binding sites. ((**S. Levy**, K. Agam, H. Cohen and B. Minke)) Dept. of Physiology, Boston Univ. Sch. Med., Boston, MA 02118 and Dept. of Physiology, Hadassah Med. Sch., Hebrew Univ., Jerusalem 91120.

Invertebrate photoreceptors in general, and those of *Drosophila melanogaster* in particular, provide excellent models for elucidating intermediate steps of phototransduction. It has been shown previously that photoexcitation of *Drosophila* photoreceptors results in Ca^{2+} influx from the extracellular space in addition to Ca^{2+} release from intracellular stores (Peretz *et al.*, J. Gen. Physiol. 104:1057, 1994). Elegant studies involving the use of phototransduction-defective mutants strongly suggest that Ca^{2+} influx occurs through the so-called TRP-dependent channels. The purpose of the present experiments was to characterize calcium fluxes in *ninaC* mutants (for neither-inactivation-nor-afterpotential). The *ninaC* gene encodes two photoreceptor-cell specific molecules consisting of a myosin head domain linked to a protein kinase catalytic domain. Of importance is the fact that NINAC has properties similar to myosin, including the presence of two calmodulin binding sites. The requirement for calmodulin binding sites in phototransduction was addressed by producing transgenic flies which lacked various binding sites. We simultaneously measured the electroretinogram (ERG) and extracellular calcium concentration (Ca_o) by use of double-barreled calcium selective microelectrodes in intact flies. Illumination of wild-type (WT) *Drosophila* photoreceptors produces a transient decrease in Ca_o quickly followed by a plateau closer to dark levels. In P[$ninaC^{\Delta 8}$] transgenic flies, which lack both calmodulin binding sites, illumination caused a more sustained transient Ca_o decrease that slowly returned to dark levels, suggesting the importance of calmodulin in phototransduction and calcium homeostasis. Supported by NIH grant NS 30672.

Tu-AM-E7

PROPERTIES AND DENSITY OF A CYCLIC GMP-GATED CATION CHANNEL ON PHOTORECEPTORS OF THE LIZARD PARIETAL EYE ((J.T. Finn[1], E. Solessio[2] and **K.-W. Yau**[1])) [1]Howard Hughes Medical Institute and Department of Neuroscience, Johns Hopkins University School of Medicine, Baltimore, MD 21205; [2]John A. Moran Eye Center, University of Utah Health Science Center, Salt Lake City, UT 84132.

Photoreceptors of the lizard parietal eye, unlike rods and cones but like many invertebrate rhabdomeric photoreceptors, respond to light under dark-adapted conditions with a depolarization even though they have a ciliary photosensitive structure. Using excised-patch recordings, we have nonetheless found a cGMP-gated channel at the presumptive light-sensitive part (outer segment) of these cells. This channel resembles the rod cGMP-gated channel in its characteristics of activation by cGMP, as well as by showing a relative nonselectivity among alkali monovalent cations, a high permeability to Ca^{2+}, a high sensitivity to *L-cis*-diltiazem (half-inhibition at ca. 3 μM at +60 mV), and a negative modulation by Ca^{2+}-calmodulin. It is present at high density selectively on the outer segment of the cell (mean of 143 channels/μm^2, versus 1.37 channels/μm^2 on the inner segment), suggesting that it plays an important role in phototransduction. Because the cell's photoresponse is a depolarization, however, light most probably raises the cGMP concentration. At the same time, a possible principle emerges: that phototransductions in various ciliary photoreceptors, regardless of response polarity, uniformly employ a cGMP cascade and a cGMP-gated channel as the mechanism generating the light response, though the details can vary.

PROTEIN-DNA INTERACTION

T-AM-SymI-1 **M. T. Record, Jr., University of Wisconsin-Madison**
Interpreting the Thermodynamics of Lac Repressor - Operator Binding: Contributions of Coupled Folding, DNA Wrapping and Looping

T-AM-SymI-2 **D. Beckett, University of Maryland**
Structural and Thermodynamic Studies of the Biotin Repressor-Biotin Operator Interaction

T-AM-SymI-3 **P. Rice, National Institute of Diabetes and Digestive and Kidney Diseases**
Crystal Structure of an IHF-DNA Complex: A Protein-Induced DNA U-turn

T-AM-SymI-4 **R. Brennan, Oregon Health Sciences University**
The Structural Basis of the Allosteric Regulation of PurR-DNA Binding

Tu-AM-F1

ELECTROPHYSIOLOGICAL PROPERTIES OF RAT HOMOLOGS OF *SCN9A* AND *SCN10A* SODIUM CHANNELS EXPRESSED IN *XENOPUS* OOCTYES. ((**B.D. Koch**, L. Sangameswaran, P. Dietrich, S.G. Delgado, L.M. Fish, R.C. Herman, and J.C. Hunter)) Inst. of Pharm., Neurobiology Unit, Roche Bioscience, Palo Alto, CA 94304.

We have cloned cDNAs for rat homologs of *SCN9A* and *SCN10A* and analyzed their electrophysiological properties by expression in *Xenopus* oocytes and TEVC recording. The rat homolog of *SCN9A*, rPN1, encodes a TTX-sensitive sodium channel (IC_{50} = 4.3 ± 0.92 nM, n=4). Neither rβ1 nor rβ2 had any effect upon the inactivation kinetics of rPN1. Steady-state inactivation analysis (10s prepulses) yielded a V½ of -78 ± 1.1 mV (n=4). Analysis of activation using macropatch recordings yielded a V½ of -31 ± 3.8 mV (n=4). Three closely related rat homologs of *SCN10A* have been cloned, rPN3, rPN3A, and SNS. rPN3 encodes a TTX-resistant (IC_{50} ≥ 100 µM) sodium channel with slow inactivation kinetics (JBC 271:5953, 1996). Neither rβ1 nor rβ2 had any effect upon the inactivation kinetics, but rβ1 increased the expression of rPN3A. Steady-state inactivation analyses (10s prepulses) of rPN3 and rPN3A yielded V½s of -54 ± 2.9 mV (n=3) and -48 ± 1.8 mV (n=3), while analyses of activation using TEVC yielded V½s of 13 ± 2.3 mV (n=2) and 17 ± 1.7 mV (n=3), suggesting that these channels have very similar properties. However, a different steady-state inactivation protocol (1s prepulses followed by 5ms midpulses), yielded V½s of -33 ± 1.1 mV (n=2) and -50 ± 1.3 mV (n=4), respectively, indicating that there are some differences. Thus the rat homolog of*SCN9A* encodes a fairly conventional TTX-sensitive sodium channel, while the homologs of *SCN10A* encode unusual, TTX-resistant sodium channels.

Tu-AM-F2

TEMPERATURE EFFECTS THE VOLTAGE DEPENDENCE OF SLOW INACTIVATION OF Na^+ CHANNELS. ((**R.L. Ruff**)) Cleveland VAMC, Case Western Reserve Univ., Cleveland, OH 44106

We investigated the temperature dependence of slow inactivation (SI) and other aspects of Na^+ channel gating due to the importance of SI in membrane excitability and the abnormal temperature dependence of Na^+ channel gating in paramyotonia congenita. We improved the quality of the seal between the loose patch pipette and the membrane, the enzymatic treatment of muscle fibers and the regulation of bath temperature to enable recording of I_{Na} at multiple temperatures up to 37°C from the same membrane patch (Figure). I_{Na} kinetics are faster at 37°C compared to 19°C. An unexpected finding is that the available current is also larger at 37°C. In the figure, 19°C, $I_{Na,max}$ was 9.4 mA/cm^2 at -103 mV and 20.1 mA/cm^2 with SI removed. At 37°C $I_{Na,max}$ was 19.2 mA/cm^2 at -105 mV and 20.3 mA/cm with SI removed. Holding the membrane at depolarized potentials indicated that SI was operative at 37°C. At 37°C the steady state voltage dependence of SI is shifted about +15 mV compared with 19°C so that fewer Na^+ channels are in the slow inactivated state at the resting potential. The ability of lower temperature to enhance SI may be disturbed in some Na^+ channel disorders such as paramyotonia congenita. [Supported by the Office of Research and Development, Medical Research Service of the Department of Veterans Affairs]

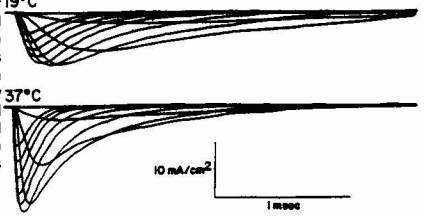

Tu-AM-F3

SLOWED SODIUM CHANNEL DEACTIVATION EXACERBATES HYPEREXCITABILITY IN PARAMYOTONIA CONGENITA. ((**D. E. Featherstone**, E. Fujimoto, P. C. Ruben)) Department of Biology, Utah State University, Logan, UT 84322-5305.

Paramyotonia congenita (PMC) is a human hereditary disorder wherein missense mutations in the skeletal muscle sodium channel lead to cold-exacerbated muscle hyperexcitability. The most common site for PMC mutations is the outer-most arginine of domain IV segment 4 (human R1448, rat R1440). We examined the rat homologs of two PMC mutants with changes at this site: R1440P and R1440C. The R->P mutation leads to the most clinically severe form of the disease. Since PMC has so far been attributed to defects in fast inactivation, we expected the R->P substitution to have a more dramatic effect on fast inactivation than R->C. Both mutants (R1440P and R1440C), however, have identical rates and voltage dependence of fast inactivation and activation. In contrast, R1440P has slower deactivation than R1440C. We show that the downstroke of the muscle action potential produces a sodium tail-current, and thus slowed deactivation opposes repolarization and therefore leads to hyperexcitability. Hyperexcitability due to slowed deactivation also predicts the temperature sensitivity of the disease, which has otherwise not been adequately explained. Supported by PHS grant R-01 NS29204 to PCR.

Tu-AM-F4

DEFICIENT SLOW INACTIVATION IN A SUBSET OF MUTANT SODIUM CHANNELS ASSOCIATED WITH PERIODIC PARALYSIS. ((**L.J. Hayward**, R.H. Brown, Jr., and S.C. Cannon)) Depts. of Neurology and Neurobiology, Mass. General Hosp. and Harvard Med. Sch., Boston, MA 02114.

Hyperkalemic periodic paralysis (HyperPP), paramyotonia congenita (PMC), and sodium channel myotonia (SCM) are dominantly inherited myotonic disorders caused by missense mutations in the skeletal muscle Na channel. These mutations impair fast inactivation or may shift activation toward hyperpolarized potentials, inducing persistent Na currents that cause muscle depolarization, myotonia, or onset of weakness. Ruff (*Biophys. J. 66*:542, 1994) proposed that slow inactivation (SI) must also be impaired to produce sustained paralysis, and Cummins and Sigworth (*Biophys. J. 71*:227, 1996) showed a destabilization of SI for a HyperPP mutant (rT698M, the rat homolog of hT704M). We tested whether additional mutant Na channels associated with paralytic phenotypes produced a defect in SI when expressed in HEK293 cells. Extent of SI was defined as the fraction of whole-cell Na current that failed to recover within 20 ms at -100 mV. Kinetics of entry to SI were measured between -70 to +20 mV using conditioning pulse durations from 20 ms to 60 s, and recovery was assessed over 10 ms to 30 s between -120 and -80 mV. The two most prevalent HyperPP mutations responsible for classic paralytic attacks (rT698M and rM1585V in the rat channel) both had clear impairment of SI. The SI defect reduced use-dependent attenuation of I_{Na} during a 50 Hz train of 5 ms pulses. However, two other mutations associated with paralysis (rT1306M [PMC] and rM1353V [HyperPP]) had intact SI, as did the non-paralytic SCM mutant, rG1299E. Model simulations showed that deficient SI, while not a requirement for stable muscle depolarization, may enhance the likelihood of paralysis and the sensitivity to elevated extracellular $[K^+]$.

Tu-AM-F5

STEADY STATE INACTIVATION AND STEADY STATE ACTIVATION IN DIFFERENT GATING MODES OF Na^+ CHANNEL ACTION

((Th. Böhle, C. Biskup, R. Koopmann*, and K. Benndorf*)) Dept. of Physiology, University of Cologne, D-50931 Cologne, and * Dept. of Physiology, Friedrich-Schiller-University, D-07740 Jena, Germany. (Spon. by C. Methfessel)

In myocardial mouse cells, cell-attached patches containing a single Na^+ channel were formed with pipette tips, which were obtained by breaking the pipette on the glass bottom of the bath chamber only seconds before giga-seal formation (ratio of outer to inner diameter of the glass tubing 4/1 or 8/1, pipette resistance up to 150 MΩ, seal resistance up to 3000 GΩ, band width 20 kHz, room temperature). Half-maximum voltage ($V_{0.5}$) and slope (k) of steady state activation (20-ms prepulses to -180 mV) were -48 mV and 6 mV in the fast inactivating (F) mode, and -61mV and 9 mV in the slowly inactivating (S) mode, respectively. At the end of 20-ms prepulses, the degree of voltage-dependent inactivation was evaluated by eliciting test currents. The peak amplitude of the test currents were normalized and fitted with the Boltzmann equation. $V_{0.5}$ and k of steady state inactivation were -90 mV and 6 mV in the F mode, and -70 mV and 13 mV in the S mode, respectively. Conclusions: Along with the slowing of macroscopic inactivation, mode switching generates shifts to more positive potentials of steady state inactivation but to more negative potentials of steady state activation and a decrease in slope of both.

Tu-AM-F6

PERSISTENT TETRODOTOXIN-SENSITIVE NA^+ CURRENT IN CULTURED HUMAN CORONARY MYOCYTES: PROPERTIES AND ROLE IN THE CONTROL OF INTRACELLULAR CA^{2+}. G. Boccara[1], JF. Quignard[1], C. Choby[1], B. Albat[2], J. Nargeot[1], G. Dayanithi[3], S. Richard[1]. CNRS, ERS 155 (1) and UPR 9055 (3); Hôpital A. de Villeneuve (2) Montpellier, Fr. (spon. by D. Mornet).

Primary cultured human coronary myocytes express a highly tetrodotoxin(TTX)-sensitive voltage-gated Na^+ current with a large sustained component (Quignard et al., 1996, Biophys. J, 70 : A320). Enzymatically isolated myocytes, from the left coronary artery of failing hearts (ischemic cardiopathy) of patients undergoing transplantation, were used in this study. Under whole-cell patch-clamp configuration, the electrophysiological properties of the Na^+ current (window current between -20 mV and -40 mV ; slow inactivation) revealed that it could play a role in the control of intracellular calcium ($[Ca^{2+}]_i$). Primary cultured myocytes were loaded with fura-2 and $[Ca^{2+}]_i$ was monitored in individual cells using digital imaging fluorescence microscopy. Exposure of cells to veratridine (100 µg/ml) and a polypeptide of *Anemonia sulcata* (AS5; 0.1 µM), two potent Na^+ channel agonists acting at distinct binding sites, induced an important increase in $[Ca^{2+}]_i$ (6 to 7 times more than basal level). The effects of veratridine and AS5 (i) were antagonized by the specific Na^+-channel blockers TTX (1 µM) and lidocaine (10 µM); (ii) required the presence of extracellular $[Ca^{2+}]_i$ and; (iii) were partially abolished in the presence of Ca^{2+}-channel blockers. Therefore, these effects may be mediated via activation of voltage-gated Ca^{2+} channels and, possibly, of a Na^+/Ca^{2+} exchanger. In addition, since AS5 acted primarily by slowing current decay with no effect on current activation, it is likely that some channels are opened at the resting membrane potential and contribute to the control of the resting $[Ca^{2+}]_i$ of human coronary myocytes.

Tu-AM-F7

VOLTAGE DEPENDENT CAPACITANCE IN PITUITARY NERVE TERMINALS. ((G.Kilic* and **M. Lindau**)). * Dept. Physiol. University of Colorado Med School, Denver, CO 80262 & Dept. Molecular Cell Research, MPI f. Medical Research, D-69120 Heidelberg, Germany.

We studied the voltage dependence of membrane capacitance in rat pituitary nerve terminals with a lock-in amplifier using an 800 Hz, 10 mV (rms) sine wave command voltage. Depolarizing and hyperpolarizing pulses with a duration of 2 to 10 s were given from a holding potential of -82 mV. In nerve terminals which showed no Na current the capacitance decreased by about 50 fF between -80 and 0 mV approaching constant levels outside this range. When a significant Na current was present, an additonal voltage dependent capacitance appeared which had a bell shaped C vs. V curve. In the potential range from -72 to -12 mV a strong positive correlation exists between the size of the Na current and the size of a capacitance change. After eliminating the part which is not due to Na current the voltage dependence was well fitted by the equation $C=\alpha Q_0/(2\cosh^2(\alpha(V_0-V)))$ with parameters α (slope factor), V_0 (voltage were capacitance reaches the peak) and Q_0 (maximum charge available to move). α and V_0 were not dependent on the size of Na current and were ~ 0.02 mV^{-1} and -40 mV, respectively. Q_0 was dependent on the size of Na current and we found ~ 15 fC/nA. These results are in good agreement with a previous frequency domain study of Na channel gating currents in squid axon [Fernandz et al. (1982) J.Gen.Physiol. 79:41]. We conclude that the bell shaped voltage dependent capacitance in pituitary nerve terminals is due to Na channel gating current.

Tu-AM-F8

NONEQUILIBRIUM RESPONSE SPECTROSCOPY OF SODIUM CHANNEL GATING. ((**M. M. Millonas** and D.A. Hanck)) University of Chicago, Chicago IL 60637.

We describe a novel set of electrophysiological protocols based on application of a rapidly fluctuating (up to 10 kHz), large amplitude (10-100 mV) voltage clamp in whole cell preparations. Because the gating responses of the channels are sensitive to subtle details in the underlying kinetics as well at to the statistical properties of the applied voltage fluctuations, the nonequilibrium response useful for probing aspects of the kinetics which are difficult to resolve by standard methods. The best new information can be expected to be obtained for fluctuations with a bandwidth equivalent to or greater than some or all of the underlying kinetic rates of the channel. Here we focus on dichotomous voltage fluctuations, a broad band, colored noise. Since this noise is Markovian, all features of the response of a proposed kinetic model to the fluctuation can be calculated in closed form and can therefore serve as a useful tool for the development of better kinetic models for voltage gated channels. We present data for the nonequilibrium response characteristics of cardiac and skeletal muscle sodium channels for varying bandwidths and amplitudes of the applied fluctuations. These involve measurements of the transient time course of the mean conductance, and the stationary probability density functions and autocorrelation functions of the conductance fluctuations at long time. We discuss how these properties can be used to test detailed channel models.

Tu-AM-F9

IDENTIFICATION OF GATING SCHEMES OF WILD TYPE AND MUTANT SODIUM CHANNELS FROM SINGLE CHANNEL RECORDINGS USING HIDDEN MARCOV MODELS.
((**S. Michalek**, H. Lerche*, N. Mitrovic*, M. Schiebe*, F. Lehmann-Horn*, J. Timmer))
Freiburger Zentrum für Datenanalyse und Modellbildung, 79104 Freiburg, and *Abteilung für Angewandte Physiologie, Universitaet Ulm, 89069 Ulm, Germany (Spon. by P.A. Iaizzo)

Hidden Markov models (HMM) can be used to investigate the functional behaviour of ion channels using patch-clamp recording techniques even if signal-to-noise ratios approach 1 (c.f. Chung et al., Phil. Trans. R. Soc. B 329:265,1990).
For a given gating model, HMM allow the maximum likelihood estimation of rate constants together with confidence intervals. The fitness of different gating schemes to the experimental data can be compared using statistical tests.
In addition, HMM yield estimators for open-/closed- time distributions and first latencies even if no idealised record is available. By calculating them for the data as well as for the model, one is able to check for consistency.
Here, we demonstrate that a comparison of identified gating schemes and rate constants for wild type and different mutants gives insights into the kinetic consequences of changes in the protein's structure.
(Supported by DFG grant HO 496/4-1 to S.Michalek).

NEUROBIOLOGY

Tu-AM-G1

ULTRAFAST TRANSMITTER RELEASE ELICITED BY CALCIUM CURRENT IN SYNAPTIC TERMINALS OF RETINAL BIPOLAR NEURONS. ((**S. Mennerick** and G. Matthews)) SUNY, Stony Brook, Stony Brook NY 11794. (Spon. by S. Mennerick)

Using high-resolution capacitance measurements, we have characterized an ultrafast component of transmitter release during depolarization in ribbon-type synaptic terminals of retinal bipolar neurons. With depolarizing pulses to 0 mV (near the peak of the calcium current/voltage relationship), the rapid capacitance increase is apparent with depolarizations as brief as 0.5 ms and plateaus at ~30 fF with a time constant of 1.5-2 ms. Using a prepulse paradigm designed to activate channels without admitting calcium, we found that the ultrafast component of exocytosis is normally rate limited by the activation kinetics of the calcium current. When calcium-current activation is experimentally accelerated, the small pool is depleted with an even-faster time constant of 0.5 ms, similar to the maximum time constant of depletion observed in flash photolysis studies at saturating intracellular calcium concentrations. After the ultrafast pool is depleted, capacitance rises with a slower time constant of ~300 ms. EGTA (5 mM) depresses the secondary capacitance rise but leaves the ultrafast phase intact. BAPTA (5 mM) depresses both components of exocytosis. With paired-pulse stimulation, the ultrafast pool, like the secondary pool, recovers from depletion with a time constant of 4-5 s. The ultrafast component may represent fusion of docked vesicles at the base of the synaptic ribbon, while the slower component represents more distal vesicles on the ribbon.

Tu-AM-G2

BOTULINUM TOXIN C1 ELIMINATES MODULATION OF PRESYNAPTIC CALCIUM CHANNELS BY GTPγS: IMPLICATION OF SYNTAXIN INVOLVEMENT IN THE G-PROTEIN MODULATION PATHWAY. ((**E.F. Stanley** and R.R. Mirotznik)) Synaptic Mechanisms Section, NINDS, NIH, Bethesda MD 20892.

N-type calcium channels are down-regulated by G-proteins, a mechanism that is believed to be a final common pathway in the control of presynaptic calcium influx and, hence, transmitter release. We tested whether G-protein-dependent modulation affects calcium channel function in an intact presynaptic nerve terminal by introducing GTPγS into the calyx of the chick ciliary ganglion while monitoring the calcium current (JNeurosci 11:985). GTPγS reduced the amplitude and slowed the activation kinetics of a pulse-evoked presynaptic calcium current, an effect that could be temporarily reversed by a preceding strong depolarization, confirming the presence of the G-protein pathway. Pretreatment with botulinum C1 (BTC1) had little effect on the calcium current or its steady-state inactivation but virtually eliminated the effect of GTPγS. This toxin has been reported to cleave both syntaxin and SNAP-25 in mammalian cells. We tested its effect in the calyx by immunofluorescence and found that in this synapse only syntaxin staining was affected (See Mirotznik and Stanley abs.). These findings suggest that linkage of the channel to the release site via syntaxin 'enables' G-protein modulation. This mechanism may ensure that release site-tethered calcium channels are selectively regulated by this second messenger pathway.

Tu-AM-G3

EXOCYTOSIS AND RAPID ENDOCYTOSIS ARE DIFFERENTIALLY AFFECTED BY THE INTRACELLULAR CALCIUM BUFFERING CAPACITY IN RAT PITUITARY MELANOTROPIC CELLS.

((**Huibert D. Mansvelder** and Karel S. Kits)) Membrane Physiology Section, Research Institute Neurosciences Vrije Universiteit, De Boelelaan 1087, 1081 HV, Amsterdam, The Netherlands. E-mail: hdmansve@bio.vu.nl

The main trigger for exocytosis in rat pituitary melanotropic cells are Ca^{2+} ions which flow into the cell through voltage gated Ca^{2+} channels. It has been shown previously that the process of rapid endocytosis in these cells is also Ca^{2+} dependent. We embarked on a study of the Ca^{2+} dependence and the relation to voltage gated Ca^{2+} channels of both processes by means of capacitance measurements. Standard whole cell voltage clamp recordings were made at 33°C. With an intracellular concentration EGTA of 50 µM 25 depolarizations from -80 mV to +10 mV at 2 Hz elicited both exocytosis and rapid endocytosis with an efficacy of ~2 and ~1.6 fF/10^6 Ca^{2+} ions respectively. When the EGTA concentration was raised to 100 and 200 µM, exocytosis was relatively unaffected, whereas the efficacy of endocytosis dropped to ~0.5 fF/10^6 ions. The efficacy of exocytosis decreased with the EGTA concentration raised to 400 µM and 800 µM EGTA. At 50 µM BAPTA efficacies of exocytosis and endocytosis were in the same range as 100 and 200 µM EGTA. These results indicate that the mobile Ca^{2+} buffering capacity of the internal medium differentially affects the efficacy of Ca^{2+} ions to stimulate exocytosis and endocytosis. Apparently, Ca^{2+} ions have to travel a substantial distance to stimulate both exocytosis and endocytosis. This distance might be larger for the process of endocytosis than for the process of exocytosis, giving rise to differential sensitivity to calcium chelators. Closer examination of the data revealed that the process of exocytosis and endocytosis are strongly correlated, and that the time constant of rapid endocytosis decreases with increasing amplitudes of exocytosis rather than with the amount of calcium that entered the cell. These data support the hypothesis that the exocytotic vesicle membrane is retrieved again rapidly, and that this process is calcium dependent.

Tu-AM-G4

FREE Ca^{2+} CONCENTRATION IS TIGHTLY REGULATED IN STEREOCILIA OF THE BULLFROG'S SACCULAR HAIR CELL. ((**Ellen A. Lumpkin** and A. J. Hudspeth)) Howard Hughes Medical Institute and Laboratory of Sensory Neuroscience, The Rockefeller University, New York, NY 10021.

By affecting the adaptation motor's slipping rate, Ca^{2+} entering a hair bundle through mechanoelectrical-transduction channels regulates the bundle's sensitivity to stimulation. For adaptation to accurately set the bundle's position of mechanosensitivity, the free Ca^{2+} concentration in stereocilia must be tightly controlled. To define the roles of Ca^{2+}-regulatory mechanisms in the hair bundle, and thus the factors influencing adaptation-motor activity, we have used whole-cell voltage-clamp recording and confocal microscopy to detect Ca^{2+} entry into and clearance from the stereocilia of hair cells dialyzed with the Ca^{2+} indicator fluo-3.

We have also developed a model of stereociliary Ca^{2+} homeostasis that incorporates four regulatory mechanisms: Ca^{2+} clearance from the bundle by free diffusion in one dimension, Ca^{2+} binding to mobile buffers that can diffuse into the soma, Ca^{2+} binding to fixed stereociliary buffers, and Ca^{2+} extrusion by pumps. To test the model's success, we have compared the predicted profiles of Ca^{2+}-fluo-3 concentration during the response to mechanical stimulation with the fluo-3 fluorescence patterns measured in individual stereocilia.

The results suggest that free and buffered Ca^{2+} diffusion cannot wholly account for the ion's observed rate of clearance from the hair bundle. Ca^{2+}-pump activity must be included for the model to accurately predict plateau concentrations of Ca^{2+}-fluo-3 during and after hair-bundle displacement. In addition, the fixed-buffer capacity influences both the concentration of Ca^{2+}-fluo-3 during stimulation and the rate at which this concentration returns to baseline after the stimulus. The best fit of the model suggests that a free Ca^{2+} concentration of tens of micromolar is attained at the adaptation motor a few milliseconds after transduction-channel opening. The free Ca^{2+} concentration substantially rises only in the upper portion of the stereocilium and quickly falls toward resting levels as adaptation proceeds.

This research was supported by HHMI and by NIH grant DC00241.

Tu-AM-G5

SITE SPECIFIC CLEAVAGE OF A FUNCTIONAL ION CHANNEL IN VIVO USING UNNATURAL AMINO ACID MUTAGENESIS. ((**P.M. England**, D.A. Dougherty, H.A. Lester)) Divisions of Biology and Chemistry, Caltech, Pasadena CA 91125 (Spon. by Charles Brokaw).

Using the *in vivo* nonsense codon supression method for incorporating unnatural amino acids into proteins, we have developed a general method for producing photochemically initiated, site specific proteolysis of proteins expressed in *Xenopus* oocytes. The photoreactive unnatural amino acid (2-nitrophenyl)glycine (NPG) was incorporated into *Drosophila* Shaker B potassium channels in the N-terminus of the protein (position 64). Photolysis of oocytes expressing mutant channels containing NPG resulted in Shaker currents in which both the rate and level of fast inactivation was significantly reduced. (NIH, CATRDRP, NRSA)

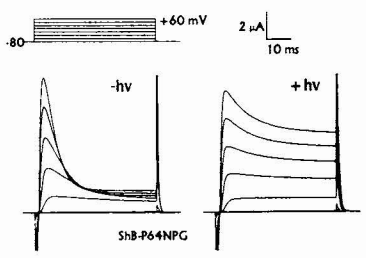

Tu-AM-G6

ESTIMATION OF LITHIUM DIFFUSION IN DENDRITIC SPINE DURING ACTIVATION OF GLUTAMATE RECEPTORS. ((**Anatolii Y. Kabakov**[1], Nikolas B. Karkanias[2] and Roger L. Papke[1,2])) Departments of Pharmacology and Therapeutics[1], and Neuroscience[2], University of Florida Medical College, J.H.Miller Health Center, Box J267, Gainesville, FL 32610-0267.

Intracellular Li^+ is important for neuronal function because it has been reported that it inhibits the myo-1-inositol monophosphatase with K_i value of 0.8 mM and other forms of second messenger coupling at higher concentrations. We have evaluated the conductance of Li^+ for ionotropic glutamate receptors using heterologous expression and two electrode voltage clamp techniques in *Xenopus* oocytes. Substitution of extracellular Na^+ for Li^+ results in an increase of the conductance for receptors composed of subunits GluR1+GluR2 by 35±9%, and for homomeric receptors composed of GluR3 by 168±2%. If we consider that an extracellular Li^+ of 1 mM concentration carries about 1% of a monosynaptic current, then our mathematical simulation of Li^+ diffusion in the dendritic spine (diameters: head - 0.6 µm, neck - 0.2 µm) suggests that one monosynaptic current with a peak of 1 nA and 4 ms decay time constant, can increase Li^+ concentration in the spine head by 2 mM and in the spine neck by 1 mM. This change in Li^+ concentration is maintained with a time decay constant about 6 ms. Application of two or more current spikes to the same spine with a 10 ms interval results in oscillation of Li^+ concentration in the head at 3 - 4 mM level. Incorporation of the limiting diffusion factors such submembrane fuzzy space and the spine apparatus in the neck results in significant elevation of Li^+ concentration in submembrane space and in the spine head, and increases the Li^+ dissipation time constant. Our results confirm that 1 mM extracellular Li^+ can inhibit the second messenger mediated coincidence detection in dendritic spines associated with the activation of glutamate receptors under physiological conditions.

Tu-AM-G7

DATABASE SCHEMAS FOR ELECTROPHYSIOLOGICAL DATASETS MAY COMPLEMENT GENOMIC AND PROTEIN SEQUENCES. ((**D. Gardner** and S.M. Erde)) Dept. of Physiology and Office of Academic Computing, Cornell University Medical College, New York, NY 10021.

Genomic or protein databases are encyclopedic and so are insufficient for determining biophysical properties of particular cells or tissues of interest. Even organ-specific cDNA-derived sequences often subsume cellular differences in expression or subcellular variations in channel targeting or density. Biophysical understanding of the role of channels in situ would be aided by universal methods for storage and display of actual datasets associated with published descriptions, analogous to those providing sequence data.

For two pilot projects addressing identified invertebrate cells and mammalian cortical sensory neurons, we have defined standards for abstract datatypes describing 11 subtypes of time series, histogram, bivariate, and multimedia electrophysiological data, as well as neuron descriptions. Physiological data require methods for storage and multiplatform search, access, and display distinct from those for ASCII-coded amino acid or nucleotides. In our design, clients use HTTP protocols to search object-oriented datasets for server-side controlled-vocabulary metadata annotations. Data objects incorporate Java methods for automatic platform-independent data delivery and display. Such standards for archiving and delivery of actual datasets, along with the development of databases for their free distribution, may additionally facilitate linking channel protein sequence data to the display and analysis of their physiological function in specific cells.

See `http://ganglion.med.cornell.edu/`

Supported by NSF: BIR 5906171; NINDS: NS36043; and NIMH: MH/OD57153.

Tu-AM-G8

Antisense to the rodent Shaker-like potassium channel Kv1.1 alters memory without effecting LTP.

((**Noam Meiri**[‡], Carla Ghelardini[*], Giuseppina Tesco[‡], Nicoletta Galeotti[*], Dennis Dahl[‡], Daniel Tomsic[‡], Sebastiano Cavallaro[‡], Alessandro Quattrone[#], Sergio Capaccioli[#], Alessandro Bartolini[*], Daniel L. Alkon[‡])). [*]Dept. of Pharmacology, and [#]Institute of General Pathology, University of Florence, Florence, Italy. [‡]LAS/NINDS, NIH, Bethesda, MD 20892, USA.

The genetic approach to study the physiological role of proteins in memory consolidation have been used extensively in recent years, but both *Drosophila* mutants and transgenic mice studies have been criticized for having developmental effects and hence might affect normal brain fine architecture. In this project we used a new genetic approach, reversibly inhibiting a potassium channel in the mature rodent brain by intracerebral injection of antisense. In order to lengthen the half life of the antisense and to increase its cellular uptake we modified the phosphodiester backbone and co-incubated it with cationic lipids. These two modifications enabled us to inject the antisense every 48 hr so that the antisense reached its expected brain targets. Since potassium channels in general and the Shaker family in particular have been implicated in memory we inhibited the potassium channel Kv1.1. We report that repeated intracerebroventricular injection of antisense oligodeoxyribonucleotides to Kv1.1 mRNA, which codes for late rectifying K^+ channels, indeed reversibly blocks memory, but not learning of two rodent species, i.e. rat spatial memory tested in the water maze and mouse passive avoidance conditioning. Since LTP has been proposed as a model for learning we checked it in the rats injected with the antisense. The memory blockade occurred in the absence of any measured alteration of LTP recorded both from the CA1 and dentate gyrus regions of the rat hippocampus. Action potentials however recorded intracellulary in the dentate gyrus do show the expected effects of K^+ blockade (no AHP, etc.). Therfore, the memory inhibition may be due to K^+ channel blockade but not to LTP

Tu-AM-H1

ENHANCED CALCIUM RELEASE AND REMOVAL ACTIVITIES IN MOUSE SKELETAL MYOTUBES CULTURED IN LOW SERUM. ((**N. Suda**, R.T. Dirksen, and K.G. Beam)) Dept. Anatomy & Neurobiology, Colorado State Univ. Fort Collins, CO 80523. (Spon. by K.G. Beam)

In adult skeletal muscle, sarcoplasmic reticulum (SR) Ca release induced by depolarization (depo) stops immediately after repolarization (repo). In mouse (129/ReJ) skeletal myotubes cultured in 10% horse serum, however, the onset and the rate of decay of cytoplasmic Ca concentration ([Ca]i) after repo are much slower than in adult muscle (Garcia & Beam, J.G. Physiol. 103, 107, 1994). Because some growth factors appear to inhibit maturation of the mechanism responsible for excitation-contraction coupling (Marks et al., J. Cell Biol. 114, 303, 1991), we investigated the effects of low serum-culturing on voltage-gated Ca transients. Combined patch-clamp and Fluo-3 measurements were performed on mouse myoballs cultured either in 0.5 or 10% serum. Patch-pipettes contained 0.1 mM EGTA and 0.4 mM Fluo-3 as Ca chelators. Cells cultured in low serum had increased rate of fluorescence change (ΔF) upon depo, increased rate of decay of ΔF upon repo, and increased ΔF/F (F: basal fluorescence) (**A**) compared to those obtained from the cells cultured in 10% serum (**B**). The immediate decay of ΔF/F in low serum myoballs upon repo allows us to estimate SR Ca release flux. Supported by HFSP to NS and NIH(NS24444) to KGB.

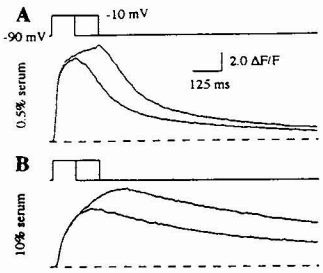

Tu-AM-H2

RISC IS PROMINENT IN MATURE SKELETAL MYOTUBES. ((**N. Suda**[1], A. Gonzalez[1], T. Tanabe[2], and K.G.Beam[1])) [1]Dept. Anatomy & Neurobiology, Colorado State Univ. Fort Collins, CO 80523; [2]Dept. Pharmacology, Tokyo Medical and Dental Univ. Faculty of Medicine. (Spon. by T. Tanabe)

Combined patch-clamp and Fluo-3 measurements were performed on mouse (129/ReJ) skeletal myotubes to investigate the effect of horse serum concentration on RISC (repolarization-induced stop of caffeine contracture). Patch-pipettes contained 0.1 mM EGTA and 0.4 mM Fluo-3 as Ca chelators. When myotubes were cultured in > 5% serum for < 7 days after initiation of fusion, RISC was not prominent and the Ca store was almost completely depleted by several exposures to 10 mM caffeine (Caf). However, myotubes cultured in 0.5% serum exhibited both RISC (**A**) and robust Ca release responses to repetitive exposure to Caf. Because Ca release and Ca removal appear to be enhanced when cells are cultured in low serum (see the companion Abstract), RISC seems to be a feature of mature skeletal muscle. The result also suggests that RISC is not present under conditions where the Ca store is easily depleted or Ca removal activity is reduced. RISC was not present in dysgenic mouse myotubes (**B**) cultured either in > 5% or 0.5% serum, supporting the idea that RISC is due to closure of the RyR through an interaction with the dihydropyridine receptor (DHPR; Suda, J. Physiol. 486, 105, 1995). These lines of evidence provide the basis for investigating the role of the DHPR in closing the RyR-Ca release channel. Supported by HFSP to NS and NIH (NS24444) to KGB.

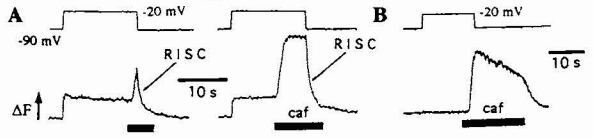

Tu-AM-H3

RISC IS DUE TO CLOSURE OF THE RYANODINE RECEPTOR (RYR) GATED BY BOTH VOLTAGE AND CALCIUM. ((**N. Suda**[1,2] and W. Stühmer[2])) [1]Dept. Anatomy & Neurobiology, Colorado State Univ. Fort Collins, CO 80523; [2]Max-Planck-Institut für Exper. Medizin. Göttingen, FRG. (Spon. by N. Suda)

Combined patch-clamp and Fura-2 measurements were performed on rat skeletal myotubes to investigate the mechanism that underlies RISC (repolarization-induced stop of caffeine-contracture; Suda & Penner, PNAS 91, 5725, 1994). RISC is not due to Ca store depletion for the following reasons: (a) the caffeine (Caf; 10 mM) transient (CafT) was terminated by repolarization (repo) even when the preceding depolarization (depo) barely induced a detectable Ca transient (CaT), (b) both voltage-gated Ca release (VOCR) and Ca-induced Ca release (CICR) activity were preserved during the decay of the CafT, (c) repo terminated CafTs at all stages, (d) VOCR evoked immediately after RISC was not reduced compared to that following a long quiescent period, (e) [Ca]i attained after a partial repo to -30 mV (from -20 mV) was elevated in the presence of Caf, whereas repo to lower voltages (< -50 mV) terminated the CaTs in the presence of Caf, and (f) RISC was inhibited in the presence of low [Mg]i (0.35 mM) and 20 mM Caf which promote store depletion. 10 mM Caf shifted the voltage-dependence (Vd) of CaTs 15-20 mV toward more negative potentials without affecting basal [Ca]i. It is unlikely that the site of Caf action is at the voltage sensor for the following reasons: (a) the decay of [Ca]i during maintained depo, which is strictly dependent on voltage and is faster at stronger potentials, did not shift toward negative potentials, (b) the activation rate of CaTs evoked by depo to -50 mV was slow, and repo occasionally failed to terminate the CaTs, (c) low [Mg]i mimicked the effects of Caf on the Vd of CaTs, and (d) during a weak depo, CafTs exhibited slow onset. Because of this slow onset, it is unlikely that Caf increases the ability of the charge movement (CHM) to open the RyR. Thus, Caf enhanced CaTs by means of CICR. It is also unlikely that the Ca-dependent component of CHM is responsible for RISC because CafTs during weak depo abruptly decay to basal level upon removal of Caf. Supported by HFSP to NS.

Tu-AM-H4

TWO TYPES OF ELEMENTARY CALCIUM RELEASE EVENTS IN SKELETAL MUSCLE REVEALED WITH CONFOCAL MICROSCOPY ((**N.Shirokova** and E.Rios)) Rush University School of Medicine, Chicago, IL 60612.

Ca^{2+} release elicited by low voltage depolarizations comprises resolvable discrete events (Tsugorka et al., 1995). It has been suggested that discrete release events (sparks) of similar amplitude are activated by T membrane voltage sensors through two mechanisms, one direct and the other mediated by Ca^{2+} (CICR, Klein et al, 1996). Cut frog semitendinosus fibers were voltage-clamped in a 2-Vaseline gap. The Ca^{2+}-related fluorescence of fluo-3 (100μM) was line-scanned with a confocal microscope. The amplitude of visually selected Ca^{2+} sparks elicited with low voltage pulses was 180 nM. Stationary noise analysis of [Ca^{2+}] gradients from individual triads was consistent with an elementary event of 164±21 nM. The fibers were subjected to two inhibitory drugs. 2 μM extracellular D600, combined with depolarization ("paralysis"), inactivated voltage sensors by about 90% (evaluated with charge movement). This intervention abolished sparks without completely eliminating Ca^{2+} release. The loss of sparks was more complete at lower test depolarizations. In agreement with the visual impression, noise analysis yielded an elementary event amplitude of 45±11 nM in D600. Tetracaine at 100 μM (a dose that inhibits CICR) eliminated sparks completely, reversibly and in a voltage-independent manner. This indicates that all sparks involve CICR. The release left in tetracaine had low stationary noise, consistent with elementary events of lower amplitude (54±6 nM). Because they are revealed by two drugs of very different mechanism, the lower amplitude events may correspond to a second physiological type of release, perhaps controlled directly by the voltage sensors. (Supported by NIH).

Tu-AM-H5

I_{Ca} IS IMPORTANT IN EC COUPLING IN DEVELOPING CULTURED EMBRYONIC AMPHIBIAN SKELETAL MUSCLE CELLS ((Ruth Cordoba-Rodriguez, Hugo Gonzalez-Serratos, Donald R. Matteson and Monika Rozycka)) Department of Physiology, University of Maryland School of Medicine, Baltimore, Maryland 21201

Adult frog phasic skeletal muscle cells have slow inward calcium currents (I_{Ca}) with no obvious role in excitation-contraction (EC) coupling. We have found that embryonic skeletal myocytes are capable of contracting in the early stages of development, at the time when the T-system and the SR may not be fully developed. Contractions could then be triggered at this stage by Ca^{2+} flowing into the cells through I_{Ca}. The present experiments were undertaken to test the hypothesis that I_{Ca} may have a role in EC coupling during early stages of skeletal muscle cell development.

This study was carried out in embryonic skeletal myocytes from *Xenopus laevis* cultured for 1-15 days. We recorded I_{Ca} with the patch-clamp technique and, Ba^{2+} as the carrier. Cell capacitance and current density indicated that I_{Ca} and total membrane area increase with time, reaching a plateau at around days 12-15. Cytosolic Ca^{2+} changes were observed from fluorescence images. While $[Ca^{2+}]_i$ increased continuously during 700 ms depolarizing pulses in young cells, older cells showed an early $[Ca^{2+}]_i$ rise followed by a steady lower $[Ca^{2+}]_i$. In young cells $[Ca^{2+}]_i$ did not increase when the cells were field stimulated in the presence of 10^{-3} M $[Ca^{2+}]_o$ while 1-week-old cells showed an increase in $[Ca^{2+}]_i$. We studied the SR functional development by measuring contracture thresholds and $[Ca^{2+}]_i$ in response to caffeine. Young cells responded to higher caffeine concentrations than older cells. Development of the T-tubular and SR membranes was investigated with fluorescence confocal microscopy. One-day-cultured myocytes are devoid of T-tubular membrane, except for short and sparse invaginations. Within 3 days, a T-tubular system forms and continues to grow until day 12 in culture. The SR is present in the periphery of the cell from day one. At this stage the SR is scanty but more abundant than the T-tubules and does not form a particular pattern. The longitudinal and transverse pattern of the SR forms within two weeks as a complex and highly dense structure. Our experiments support the hypothesis that in the early stages of development, calcium influx through I_{Ca} may be needed to trigger contraction, at the time when the SR is underdeveloped. Supported by NIH grant RO17048.

Tu-AM-H6

VOLTAGE GATING KINETICS OF SKELETAL MUSCLE CALCIUM RELEASE INVESTIGATED WITH SUPERCHARGING PULSES

((A.M. Kim and J.L. Vergara)) Department of Physiology, UCLA, Los Angeles, CA 90095

In skeletal muscle, the voltage dependence of Ca^{2+} release from the sarcoplasmic reticulum has traditionally been studied by voltage-clamping single fibers in the absence of active conductances (e.g., Na^+). However, characterization of the release process under these conditions reflects the constraints implicit in charging the significant capacitance of the transverse tubule system (TTS) through a resistance in series. We applied supercharging command pulses to attain fast step depolarizations of the TTS at rates which approach those of Na^+-mediated TTS action potentials. Single frog skeletal muscle fibers were stained with 200-400μM of the low-affinity fluorescent Ca^{2+} indicator OregonGreen 488 BAPTA-5N (OGB-5N) and voltage-clamped in a triple vaseline-gap chamber at 18°C. Epifluorescence illumination was restricted to a semicircular segment located at the edge of the fiber (10-15% of focal plane fiber area). OGB-5N transients were recorded with a PIN photodiode in response to voltage step pulses of varying lengths (5-50ms) and amplitudes, and the equivalent supercharging pulses. These latter pulses were optimized to ensure fast voltage steps in the TTS as reported by *weighted-average* potentiometric fluorescence records from the edge of the fiber. OGB-5N transients elicited by step commands showed prominent onset delays that decreased with increasing voltages. In contrast, the range of these delays in transients evoked by supercharging pulses was markedly diminished. Furthermore, supercharging accelerated the gating of the release process such that the maximum rate of Ca^{2+} release was attained up to 5 ms earlier (at 60 mV) than in transients obtained from step pulses. Surprisingly, peak rates of release were not significantly different between the two types of command pulses over the range of voltages tested (40-180mV). Our results suggest that supercharging pulses establish TTS voltages at rates that unveil an accurate portrait of the fast gating kinetics of the Ca^{2+} release process. Supported by NIH AR25201.

Tu-AM-H7

EFFECT OF PARTIAL SARCOPLASMIC RETICULUM (SR) CALCIUM DEPLETION ON SR CALCIUM RELEASE IN FROG CUT MUSCLE FIBERS EQUILIBRATED WITH 20 mM EGTA. ((P.C. Pape, D.-S. Jong, & W.K. Chandler)) *Department of Cellular and Molecular Physiology, Yale University School of Medicine, New Haven, CT 06510.*

After SR Ca release has been activated by depolarization, it can be turned off by repolarization. The effect of SR Ca content ($[Ca_{SR}]$) on the turn-off was studied by varying resting $[Ca_{SR}]$ ($[Ca_{SR}]_R$), and using the EGTA-phenol red method to measure Ca release and $[Ca_{SR}]$ (Pape et al., 1995, *J. Gen. Physiol.*, **106**, 259-336; 13-15°C). With a single action potential, Ca release decreased from about 200 to 100 μM when $[Ca_{SR}]_R$ was reduced from 1000 to 200 μM. The associated 2-3 fold increase in fractional amount of Ca released from the SR was caused by a prolongation of release; the time constant associated with the final half of release was increased from 1-2 to 10-15 ms. These effects of reduced $[Ca_{SR}]$ on Ca release were also observed with a brief stimulation (10-12 ms to ~20 mV) in voltage-clamped fibers, in which currents from intramembranous charge movement (Q_{cm}) could be measured. The amount and kinetics of ON Q_{cm} were little affected by reducing $[Ca_{SR}]_R$ from 1000 to 200 μM. Although the amount of OFF Q_{cm} was also little affected, its kinetics became progressively slowed; the final time constant increased 2-4 fold and, at $[Ca_{SR}]_R = 200$ μM, was similar to that of Ca release. Thus, the slowing of the turn-off of Ca release appears to be caused, at least partially, by a slowing of the kinetics of OFF Q_{cm}. Other processes, such as a reduction in Ca inactivation of Ca release, may also be involved. *Supported by NIH grant AR-37643.*

Tu-AM-H8

EFFECT OF EXTERNAL ANION ON CALCIUM RELEASE IN FROG SKELETAL MUSCLE FIBERS. ((**Chiu Shuen Hui**)) Dept. of Physiol. and Biophys., Indiana Univ. Med. Ctr., Indianapolis, IN 46202, USA.

Ca transient was measured in stretched cut frog twitch fibers with the double Vaseline-gap voltage clamp technique. The end-pool solution contained primarily Cs-glutamate, 20 mM EGTA plus added Ca (nominal free $[Ca^{2+}]$ was 50 nM), and ApIII as the Ca indicator. The center-pool solution contained mostly TEA^+ and either Cl^- or an impermeant anion. The rate of Ca release computed from the ApIII absorbance change showed an early peak (Rel_p) followed by a more-or-less maintained level (Rel_m). For each center-pool solution, Rel_p was plotted against membrane potential, corrected for the change in fiber condition, and fitted with a Boltzmann distribution function. The maximum Rel_p in a Cl^- solution was 2-3 times as large as those in impermeant anion solutions (98±6 μM/ms in Cl^- vs 47±3 μM/ms in $CH_3SO_3^-$, 43±10 μM/ms in gluconate, and 34±6 μM/ms in SO_4^{2-}). There was no apparent shift in the Rel_p vs V relationship when the anion was changed. The release waveform was compared in the Cl^- and $CH_3SO_3^-$ solutions at –30 mV. In Cl^-, Rel_p was 26 μM/ms and Rel_m was 10 μM/ms. After Cl^- was replaced by $CH_3SO_3^-$, Rel_p was 21 μM/ms and Rel_m was 14 μM/ms. This effect of $CH_3SO_3^-$ was mostly reversible. If the existence of the peak was due to Ca-inactivation of Ca release, then the inactivation was 62% in Cl^- and 33% in $CH_3SO_3^-$ for that pair of traces. If the peak was generated by Ca-induced Ca release, then $CH_3SO_3^-$ appeared to decrease Rel_p and increase Rel_m. (Supported by NIH NS–21955).

Tu-AM-H9

NUCLEAR IP_3 RECEPTORS AND CALCIUM SIGNALS IN CULTURED SKELETAL MYOTUBES. ((**E. Jaimovich** and J. L. Liberona)) Departamento de Fisiología y Biofísica, Facultad de Medicina, Universidad de Chile and Centro de Estudios Científicos de Santiago casilla 16443, Santiago 9, Chile.

Calcium images by confocal microscopy and binding of ^{3}H-ryanodine and ^{3}H-IP_3 were studied in both rat myoblasts and myotubes in primary culture. Upon potassium depolarization, 6-10 day old rat myotubes dysplay both a fast propagated $[Ca^{2+}]$i signal that spans the whole cell in tenths of a second and a much slower (3-20 μm/s) $[Ca^{2+}]$i wave; propagation being dependent on the presence of nuclei. Only the fast signal induced contraction in able myotubes; long lasting calcium fluorescence was much higher in nuclear regions. Incubation with 1 μM ryanodine abolished the fast signal and prevented propagation of the slow, long lasting signals to regions devoid of nuclei. The presence of possible Ca release channels was studied as expresion of ryanodine and IP_3 receptors. Rat myoblasts do not express IP_3 receptors and they reach 4 pmol/mg protein (Kd = 100 nM) in 7 day old myotubes while ryanodine binding reaches 1.2 pmol/mg protein (Kd = 11 nM). Ryanodine receptors were located in a microsomal light membrane fraction while IP_3 receptors were preferentially found in the heavy nuclear fraction. These findings, together with the reported increase in the mass of IP_3 upon potassium depolarization in these cells, suggest a role for at least two types of intracellular calcium release channels in skeletal muscle cells; ryanodine receptors mediating fast calcium transients and IP_3 receptors mediating nucleoplasmic calcium signals. Financed by MDA and European Economic Comunity.

Tu-AM-H10

TIME COURSE OF SARCOPLASMIC RETICULUM Ca^{2+} RELEASE DETERMINED FROM THE ACTIVATION OF DISCRETE Ca^{2+} RELEASE EVENTS ((M.G. Klein, A. Lacampagne, M.F. Schneider)) Dept. of Biochem. and Mol. Biol., Univ. of Maryland School of Med., Baltimore MD 21201

Discrete Ca^{2+} release events were monitored as localized changes in fluorescence of the Ca^{2+}-indicator, fluo-3, in frog skeletal muscle fibers using a confocal microscope in line-scan (*x* vs *t*) mode (Klein et al, 1996, Nature, 379:455). Single cut fibers were voltage-clamped at a holding potential of 0 mV in a double Vaseline-gap chamber. A small fraction of the voltage sensors for SR Ca^{2+} release was reprimed by briefly repolarizing the fiber to -90 or -120 mV. The fiber was then depolarized in order to activate the reprimed voltage sensors, and to activate Ca^{2+} release from ryanodine receptor Ca^{2+} release channels. This protocol allowed the detection and measurement of discrete events at all voltages within the range of activation of Ca^{2+} release. The amplitude and spatio-temporal extent of individual release events were found to be independent of repriming time, test pulse voltage and time during the test pulse. A histogram of the latency of such stereotyped events in all sarcomeres during the depolarizing test pulse thus gives the time course of Ca^{2+} release event activation, and is proportional to the rate of Ca^{2+} release from the sarcoplasmic reticulum (SR). For test depolarizations to 0 mV the observed latency plot exhibited a large early peak, followed by a decline to a much lower maintained steady level. This method for determining the rate of SR Ca^{2+} release is independent of assumptions concerning indicator kinetics and properties of myoplasmic Ca^{2+}-binding proteins. Supported by NIH (R01-NS23346 and R01-AR44197).

LIPID-PROTEIN INTERACTIONS

Tu-AM-I1

PEPTIDE-LIPID INTERACTIONS IN LANGMUIR MONOLAYERS. A NOVEL APPROACH TOWARD STRUCTURAL AND THERMODYNAMIC ANALYSES. ((**Gerhard Schwarz** and Susanne E. Taylor)) Department of Biophysical Chemistry, Biocenter of the University, CH 4056 Basel, Switzerland.

Lipid monolayers at the air/water interface with added peptide or protein provide useful model systems to study relevant physicochemical membrane properties. We have recently developed a novel method of processing conventional surface pressure versus area data allowing a quantitative analysis of the possible non-negligible desorption into the aqueous subphase experienced by a largely insoluble monolayer. This has been successfully applied to single components such as the putative HIV-1 gp41 fusion peptide [Schwarz and Taylor (1995) *Langmuir* **11**, 4341], the bee venom factor melittin [Wackerbauer, Weis and Schwarz (1996) *Biophys. J.* **71**, 1422] and the lipid POPC [Schwarz, Wackerbauer and Taylor (1996) *Colloids Surfaces A* **111**, 39]. In the latter case it turned out that in contrast to common belief there may be a practically significant bulk volume partitioning. We have now expanded our approach to the HIV fusion peptide when it interacts with a preformed POPC monolayer. By means of the proposed generally applicable procedure the molar fraction of incorporated peptide and its molecular area can be determined separately from pressure-area isotherms without any additional information. Pertinent results will be presented demonstrating substantial changes of the interfacial peptide to lipid ratio ("binding" degree) depending on the lateral pressure. Also we observed rather pronounced effects on the molecular area requirements.

Tu-AM-I2

MOLECULAR DYNAMICS SIMULATIONS OF THE INDIVIDUAL A, B, AND THE A:B PAIR OF α-HELICES FROM BACTERIORHODOPSIN IN EXPLICIT BILAYER AND MICELLE ENVIRONMENTS ((**T.B. Woolf**)) Department of Physiology, Johns Hopkins University, School of Medicine, Baltimore, MD 21205

Molecular dynamics computer calculations to compare the energetic and motional behavior of α-helices in bilayers and micelles are described. The micelle simulations use 60 SDS micelles to solvate both the individual A, B and the A:B pair of helices from bacteriorhodopsin. The bilayer simulations used both DMPC and DPPC to examine the same helices in a planar geometry. The micelle simulations were initiated with the aid of a library of SDS conformations generated from simulations of MacKerell (*J. Phys. Chem.* **99**:1846-1855). Individual SDS molecules were randomly selected and placed around the peptide(s). A water overlay and sodium counterions brought the total micelle simulations to about 20,000 atoms. Gradual minimization and restrained equilibration relaxed the initial structures. The results are analyzed in terms of interactions energies, hydrogen bonding, dihedral changes, and average structures. Particular care in the analysis was made to compare NMR observables from the two types of environments. These results are discussed in regard to the choice of the micelle environment as a mimic for the bilayer.

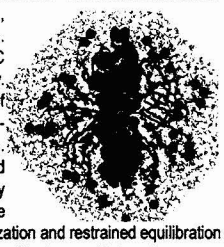

Tu-AM-I3

DEPTH-DEPENDENT FLUORESCENCE QUENCHING IN MEMBRANES: EVALUATION OF SYSTEMATIC ERRORS.
((**A.S. Ladokhin** and S.H. White)) Department of Physiology & Biophysics, University of California, Irvine, CA 92697.

Depth-dependent fluorescence quenching in membranes plays an increasingly important role in the determination of the low resolution structure of membrane proteins. Parallax Method, **PM**, (Chattopadhyay and London 1987. *Biochemistry* **26**:39) and Distribution Analysis, **DA**, (Ladokhin 1993. *Biophys. J.* **64**:A290; Ladokhin and Holloway 1995. *Biophys. J.* **69**:506) are utilized to quantitate such quenching caused by lipid-attached bromines or spin labels in order to extract the information on membrane penetration. We present a systematic comparison of the two methods based on their ability to describe various experimental and simulated data. We examined the information provided by DA and PM with respect to (1) transleaflet quenching, (2) incomplete binding, (3) uncertainty in the fluorescence in non-quenching lipid, (4) uncertainty in the local concentration of quenching lipids (due to protein shielding), and (5) existence of multiple conformations of membrane-bound protein. In its present form, PM is insensitive to (2) and (3). One can improve PM's performance against effects of (4) and (5), but not (1), by introducing a third parameter, related to quenching efficiency, that uncouples width and area of the quenching profile. Because DA utilizes a smooth fitting function in addition to three fitting parameters its solutions are largely unaffected by all of the examined factors. GM-46823, AI-22931.

Tu-AM-I4

MOLECULAR DYNAMICS SIMULATION OF THE PGHS-1 MONOTYPIC MEMBRANE PROTEIN ANCHOR DOMAIN IN A PHOSPHOLIPID BILAYER.
((**M. Nina** and B. Roux)) GRTM. Department of Chemistry, University of Montreal, Montreal, Quebec, Canada H3C 3J7

Prostaglandin H_2 synthase-1 (PGHS-1) catalyses the synthesis of prostaglandin H_2 from arachidonic acid in two consecutive steps: a cyclooxygenase activity involved in converting arachidonic acid to PGG_2 and a hydroperoxydase activity that reduces the hydroxyl group of PGG_2 to PGH_2. Based on the X-ray structure (Picot et al., 1994), it is suggested that membrane insertion is mediated by a motif comprising 3 amphiphilic helices (A,B,C) which lies parallel to the membrane plane. However the exact location of the protein relative to the bilayer surface is not known.

In this work, a macroscopic approach for the evaluation of protein solvation energies using computer calculations was used to help in determining a plausible orientation for the PGHS anchor domain relative to the membrane. The electrostatic contribution to the free energy of solvation is obtained by solving numerically the Poisson-Bolzmann equation for the protein embedded in a low dielectric medium and in water. The membrane is represented as a single slab immersed in a solvent region. The hydrophobic effect is calculated from the solvent exposed area. Based on the minimum free energy of solvation of PGHS-1 anchor domain relative to the membrane, a model system for MD simulation comprising the binding motif, DMPC molecules and water molecules was constructed. A molecular dynamics simulation of PGHS-1 membrane anchor domain in an explicit bilayer was generated to study the details of the lipid-protein interactions at the microscopic level.

Tu-AM-I5

HYDROPHOBICITY MODULATES INTEGRATION AND CONFORMATION OF PEPTIDES IN MEMBRANES
((**Li-Ping Liu**, Chen Wang, Natalie K. Goto and Charles M. Deber*)) Division of Biochemistry Research, Hospital for Sick Children, Toronto M5G 1X8; Department of Biochemistry, University of Toronto, Toronto M5S 1A8, Ontario, Canada.

Translocation of proteins into and across biological membranes is essential for many cellular processes. Thus, understanding the mechanism of protein insertion into membranes is crucial in order to gain direct insight into these processes[1]. We describe a model peptide approach which allows the systematic examination of the interaction of peptides with membranes. Previous studies with Ala-based model peptides (Lys-Lys-Ala-Ala-Ala-X-Ala-Ala-Ala-Ala-Ala-X-Ala-Ala-Trp-Ala-Ala-X-Ala-Ala-Ala-Lys-Lys-Lys-Lys-amide, X = A, F, V, T, S, and G, respectively) have shown that maintaining a 'threshold hydrophobicity' seems to be important for peptides to integrate successfully into membranes in a stable α-helical conformation[2]. In the present work, we expand the original library to include peptides containing 'guest' residues of most of the other 20 commonly-occurring amino acids, and by α-aminoisobutyric acid (Aib). Results describing the conformation(s) of model peptides in membrane-mimetic environments (including micelles, organic solvents and lipid vesicles) will be presented, along with a discussion of specific effects noted for aromatic residues[3] and a consideration of the general implications of the 'threshold hydrophobicity' hypothesis.

[1]C.M. Deber & N.K. Goto, *Nature Struct. Biol.* 3, 815-818 (1996). [2]L.-P. Liu et al. *Biopolymers* 39, 465-470 (1996). [3]W.C. Wimley & S.H. White, *Nature Struct. Biol.* 3, 842-848 (1996).

Tu-AM-I6

HEAT-, COLD- AND CHEMICAL UNFOLDING OF HUMAN APOLIPOPROTEIN C-1.
((**O. Gursky**)) Biophysics Dept., Boston University School of Medicine, Boston MA,02118

Human plasma apolipoprotein C-1 (6.6 kD), the smallest of the exchangeable apolipoproteins, is an important constituent of VLDL and HDL. To understand the basis for conformational adaptability of C-1 that is essential for its functions and transfer among VLDL and HDL, we used CD to monitor chemical and thermal unfolding of lipid-free apoC-1 in a broad range of temperatures (-10 ° to 95 °), protein concentrations (0.01-0.22 mg/ml) and solvent ionic conditions. At pH7, the far-UV CD melting curves show that C-1 is most stable at ~25 ° and unfolds reversibly both upon heating and cooling from 25 °. At acid pH, when C-1 is <30% α-helical but does not self-associate, no cooperative thermal transitions were observed. At pH7, the concentration-dependence of the thermal transitions is consistent with disassociation of C-1 oligomers upon unfolding. Consistent with the earlier studies, the mean α-helical content is ~33% for monomers at 0.01 mg/ml C-1 and rapidly increases upon self-association at >0.02 mg/ml C-1. Gdn HCl unfolding experiments indicate low stability for C-1 monomer at pH7 in 0.01M salt, $\Delta G(25\,^{\circ})=0\pm0.4$ kcal/mol, implicating that monomeric C-1 is only 34-66% folded. A more complete folding is induced by self-association. Marginal stability of C-1 monomers and oligomers at near-physiological solvent conditions, evident from the close proximity of the heat- and cold-unfolding transitions, suggests that *in vivo* C-1 co-transfers in complex with other proteins and/or lipids. Low-temperature unfolding indicates the importance of hydrophobic interactions in the stabilization and self-association of C-1.

Tu-AM-I7

MEMBRANE ASSEMBLY OF THE 16-KDA V-ATPASE PROTEOLIPID SUBUNIT FROM SPIN-LATTICE RELAXATION ENHANCEMENTS IN SPIN LABEL ESR.
((T. Páli[1], M. E. Finbow[2], and D. Marsh[1])) [1]Max-Planck-Institut für biophysikalische Chemie, Abteilung Spektroskopie, Am Fassberg, D-37077 Göttingen, Germany and [2]Beatson Institute for Cancer Research, Garscube Estate, Bearsden, Glasgow, G61 1BD, U.K.

The 16-kDa proteolipid from the hepatopancreas of *Nephrops norvegicus* belongs to the class of channel proteins that includes the proton-translocation subunit of the vacuolar ATPases. It may be isolated in native membranes as 2-D arrays that have been modelled as hexameric assemblies of 4-helix transmembrane bundles. Electron spin resonance (ESR) spectroscopy was used to study the state of assembly in the membrane from the lipid-protein interactions with lipid spin labels and measurements of spin-spin interactions with the spin-labelled protein. Saturation transfer ESR intensities of the labelled protein were used as a sensitive indicator of spin-lattice relaxation. The specific sites of spin-labelling are the unique cysteine Cys54 in helix 2, labelled with nitroxyl maleimide, and the essential glutamate Glu140 in helix 4, labelled by a nitroxyl analogue of dicyclohexylcarbodiimide (DCCD). Spin-lattice relaxation enhancements by aqueous paramagnetic Ni^{2+} ions determine the relative vertical locations of these spin-labelled residues in the membrane. Both reside within the hydrophobic region. Spin-spin interactions between spin-labelled lipids and spin-labelled protein probe the accessibility of these residues to the lipid phase; both are accessible. Spin-spin interactions as a function of labelling level are sensitive to the oligomer size and are consistent with a hexamer. The results can be used to test and refine the molecular model of the channel assembly in terms of helix location and orientation. In particular, the DCCD-reactive site essential to proton translocation appears to face the lipid.

Tu-AM-J1

MEASURED AFFINITIES BETWEEN G PROTEIN βγ HETERODIMERS AND PLC-β_1,β_2, AND β_3. ((**L.W. Runnels**, S. Scarlata, A. Morris*)) Dept. of Pharmacology* and Dept. of Physiology & Biophysics, SUNY Stony Brook, Stony Brook, NY 11794-8661.

Phosphatidylinositol-specific Phospholipase C (PLC) is divided into three classes, β,δ, and γ. The PLC-β class is regulated by heterotrimeric GTP-binding proteins (G proteins) that are made up of α and βγ subunits. G proteins of the α_q class activate PLC *in vitro* and *in vivo*. G protein βγ heterodimers from various sources also activate PLC *in vitro*, and some evidence suggests that PLC-β is also regulated by G protein βγ subunits *in vivo*. To date, G proteins of the α_q class have been shown to have only one effector, PLC-β. However, many proteins are known to be regulated by G protein βγ subunits. Thus, the specificity of G protein βγ subunits for PLC-β is in question. To better understand the regulation of PLC-β by G protein βγ heterodimers, we have measured the relative affinities of three isoforms from the PLC-β class, PLC-β_1, PLC-β_2, and PLC-β_3, to G protein βγ subunits reconstituted into large unilamellar vesicles. Using fluorescence spectroscopy, we find that the rank of relative affinities of G protein βγ subunits for PLC-βs is: PLC-β_2 > PLC-β_3 ≥ PLC-β_1. In addition, the relative affinities between the proteins appear to dictate the potency of activation of PLC-β by G protein βγ heterodimers on lipid bilayers. The possibility of dual regulation of PLC-β class by both G proteins of the α_q class and G protein βγ subunits will also be discussed.

Tu-AM-J2

DUAL COUPLING OF β_2-ADRENERGIC RECEPTOR TO G_i AS WELL AS TO G_s IN CARDIAC MYOCYTES

((R.-P. Xiao, P. Avdonin, S.A Akliter*, Y.-Y. Zhou, B. Ziman, H. Cheng, R.J. Lefkowitz†, W.J. Koch* and E.G. Lakatta)) LCS, GRC, NIA, Baltimore, MD 21224; * Dept. of Surgery, †Dept. of Medicine. and Howard Hughes Med. Insti., Duke Univ. Med. Cent. NC 27710. (Spon. by E.G. Lakatta)

An exclusive coupling between β-adrenergic receptors (βARs) and the stimulatory G protein (G_s) to activate adenylyl cyclase has been widely accepted as "dogma" of βAR signaling in native tissues. Here we demonstrate, for the first time, that β_2ARs are biochemically and physiologically coupled to inhibitory G proteins (G_i) as well as to G_s in both non-transgenic (NTG) and β_2AR overexpression transgenic mouse (TG4) hearts. In addition to G_s, β_2AR stimulation increased incorporation of a photoreactive GTP analog, [α-^{32}P]GTP azidoanilide, into α subunits of pertussis toxin (PTX)-sensitive G proteins, $G_{\alpha i2}$ and$G_{\alpha i3}$. In the absence of PTX, β_2AR stimulation was unable to augment myocardial adenylyl cyclase activity, the intracellular Ca^{2+} transient or contractility. PTX treatment unmasked a marked β_2AR-stimulated positive inotropic effect in both NTG and TG4 ventricular myocyteS. We conclude that β_2AR in murine cardiac myocytes simultaneously initiates two functionally opposite signaling pathways mediated by G_s and G_i, and that activation of the β_2AR-coupled G_i exerts a potent negative feedback on the contractile response to β_2AR stimulation. This novel signaling mechanism of β_2AR stimulation in the heart might be applicable to a broad array of G protein-coupled receptors in native tissues.

Tu-AM-J3

SEQUENTIAL BINDING OF THYROTROPIN-RELEASING HORMONE (TRH) TO THE TRH RECEPTOR: A MODEL FOR SMALL LIGAND BINDING TO G PROTEIN COUPLED RECEPTORS. ((**Anny-Odile Colson**[1], Jeffrey H. Perlman[2], Rahul Jain[3], Louis A. Cohen[3], Roman Osman[1] and Marvin C. Gershengorn[2])) [1]Mount Sinai School of Medicine, New York, NY 10029, [2]Cornell Medical College, New York, NY 10021, [3]NIDDK, NIH, Bethesda, MD 20892

Previous mutational and computational studies of the TRH receptor (TRH-R) presented evidence that four amino acids within the putative transmembrane domain (TMD) interact with TRH (pGlu-His-ProNH_2) (Laakkonen et al. Biochemistry, 1996, 35, 7651). In particular, through complementary mutations of the receptor and the ligand, we show that N110, positioned deep in the TMD, is interacting with the N-H group of the pGlu of TRH. A model of TRH-R with extracellular loops shows that access to the binding pocket is occluded, raising the question of the mechanism of TRH entry into the TMD. Complementary mutations of N289, a surface residue at the amino terminus of the third extrahelical loop, and TRH, show that N289 also interacts with the same N-H group of pGlu of TRH. To answer the question as to how these residues similarly affect binding of the ligand, molecular dynamics simulations of the complex of TRH with TRH-R were performed. Our results show that TRH cannot interact with both asparagines simultaneously and that the extracellular loops form a channel that leads to the transmembrane binding pocket. Kinetic analyses of the mutated receptors reveal that N289A affects primarily the rate of association of TRH, whereas N110A affects the rate of dissociation. Thus, TRH initially interacts with the extracellular domain and then binds within the TMD. These results, along with the computational model, are consistent with the idea that TRH initially interacts with the putative entry channel on the surface of the receptor and, by inducing a conformational change, moves into the transmembrane binding pocket.

Supported by US PHS Grant DK43036

Tu-AM-J4

BLOCKADE OF β_2-ADRENERGIC POSITIVE INOTROPIC EFFECT BY INHIBITORY cAMP ANALOG Rp-CPT-cAMP IN CARDIOMYOCYTES

((**Y.-Y. Zhou**, E.G. Lakatta, R.-P. Xiao)) LCS, GRC, NIA, Baltimore, MD 21224.

Previously we have demonstrated that responses to β_2-adrenoceptor (β_2AR) stimulation in rat ventricular myocytes differ quantitatively and qualitatively from those of β_1AR stimulation. Specifically, in contrast to β_1AR stimulation, the contractile augmentation following β_2AR stimulation develops more slowly, is dissociated from the increase in whole cell cAMP and is *not* accompanied by either a marked phosphorylation of phospholamban , a reduction in the duration of the Ca^{2+} transient or enhanced relaxation. In addition, β_2AR, but not β_1AR, is functionally coupled to pertussis toxin (PTX) sensitive G/G_o proteins. However, β_2AR also couples to G_s-adenylyl cyclase and a role for this coupling in contraction augmentation has not been definitively excluded. The aim of present work is to further examine a possible role of cAMP in β_2AR signal transduction by using an inhibitory cAMP analogue, Rp-CPT-cAMP (Rp). Cells were preincubated with 10^{-4} M Rp for 1 hr at 37°C at reduced external [Ca^{2+}] and success of loading was routinely assessed by a loss of inotropic responses to nonreceptor-stimulated adenylyl cyclase activity by forskolin. As expected, Rp blocked the inotropic effects of β_1AR stimulation elicited by norepinephrine ($5x10^{-8}$ M) plus prazosin (10^{-6}M). Surprisingly, Rp also completely abolished the responses of contraction amplitude to the β_2AR agonist zinterol (10^{-5}M and 10^{-6}M) both before (213±16%, n=12, vs 85±20% ,n=8, of control) and after PTX (245±33% , n=8, vs 91±19%, n=7, of control). Thus, cAMP signaling is required, either directly or indirectly, in mediating the β_2AR stimulated positive inotropic effect in rat cardiac myocytes, but the involvement likely differs from that of β_1AR, possibly due to differential cAMP compartmentalization or to modification by a β_2AR-coupled G/G_o pathway.

Tu-AM-J5

SPACIAL COMPARTMENTALIZATION OF Ca^{2+} SIGNALING COMPLEXES IN PANCREATIC ACINI. ((X. Xu, W. Zeng, J. Diaz and **S. Muallem**)). Univ of TX SW Med Center Dallas, Dallas, TX 75235

Imaging Ca^{2+} at high time resolution of single cells consecutively stimulated with several Ca^{2+}-mobilizing agonists revealed agonist-specific initiation site, wave pattern and propagation rate. On the other hand, repetitive stimulation with the same agonist induced Ca^{2+} waves of identical initiation site, pattern and propagation rate. The agonist-specific Ca^{2+} signaling was not due to coupling to different G proteins as inhibition of Gq by infusing IgG anti αq through a patch pipette inhibited signaling by all agonists to the same extent. The compartmentalization and specificity in signaling was corroborated by measuring the properties of Ca^{2+} signaling in agonist-competent, SLO-permeabilized cells. Measuring the effect of GTPγS and GDPβS on IP_3 production and Ca^{2+} release reveals dual role for G proteins in Ca^{2+} signaling: Regulation of PLC activity and the coupling of IP_3 production to Ca^{2+} release. Regulation of IP_3 production by G proteins was similar for all agonists. However, the ability of IP_3 generated by each agonist to release Ca^{2+} was highly agonist specific in its regulation by G proteins. These findings suggest spacial compartmentalization of Ca^{2+} signaling complexes. Each complex must include a receptor, G protein, and phospholipase C that are coupled to a specific portion of the IP_3 pool.

Tu-AM-J6

THE THREE DIMENSIONAL STRUCTURE OF THE CYTOPLASMIC FACE OF THE G PROTEIN RECEPTOR, RHODOPSIN, AND ITS INTERACTION WITH THE G PROTEIN, TRANSDUCIN. ((**Philip L. Yeagle**, James L. Alderfer, and Arlene D. Albert)) Department of Biochemistry, School of Medicine and Biomedical Sciences, University at Buffalo, Buffalo, NY 14214 and Department of Biophysics, Roswell Park Cancer Institute, Buffalo, NY 14263

No high resolution structure has been available for any G protein receptor, a many-membered family of cell surface receptors. The high resolution structures of all the cytoplasmic domains of the G protein receptor, rhodopsin, have been determined by high field multidimensional nuclear magnetic resonance. Docking of these structures with the low resolution structure of the transmembrane helical domain of rhodopsin leads to the construction of the cytoplasmic surface of rhodopsin. Interaction of this structure with the structure of the G protein suggests a molecular mechanism for the activation of the G protein by the receptor.

This work was supported by National Institutes of Health Grant EY03328 and in part by CA16056.

Tu-AM-J7

THE CONFORMATION OF THE SECOND IC-LOOP OF THE GnRH RECEPTOR CONTRIBUTES TO SIGNALING EFFICIENCY ((**F. Guarnieri**[1], L. Chi[3], V. Rodic[3], J. Ballesteros[1], H. Weinstein[1] and S.C. Sealfon[2,3])) Depts. of Physiology and Biophysics[1], Neurology[2] and Fishberg Research Center in Neurobiology[3], Mount Sinai School of Medicine, New York, NY 10029. (Spon. by Marc Glucksman)

The second intracellular loop (IC_2) of the gonadotropin-releasing hormone receptor (GnRHR) contains the sequence RPL, which has been implicated in G-protein coupling in other receptors. In GnRHR, mutation of L3.58(147)->A causes a 6-fold reduction in receptor efficiency, while the P3.57(146)->A receptor expressed poorly, but is functionally coupled to phosphoinositol hydrolysis. Little change was seen with the R3.56(145)->A mutation. To explore the conformational requirements of this region, the mutation R3.56(146)->P was done to introduce a Pro-Pro motif designed to impose conformational constraints. Unlike the R->A mutation, R->P mutation caused a 14-fold decrease in receptor efficiency. The results suggest that a specific structure of this domain is critical for efficient signaling. To determine the conformations of this domain in the wild-type and mutant receptors, computational simulations were carried out with the technique of Conformational Memories. In the less efficient R->P construct, the Pro-Pro motif restricts the conformations accessible to the loop segment. Comparison of the structures accessible to the wild-type and R3.56(145)->P mutant identifies the conformations likely to be preferred for G-protein coupling. Incorporation of these loop conformations in a receptor model indicates that in the wild-type, but not in the R3.56(145)->P mutant, the IC_2 is oriented to interact with other G-protein coupling domains. Interestingly, the analogous R->P mutation on the vasopressin V2 gene causes nephrogenic diabetes insipidus. *Supported by NIH grants DK-46943, DA-00060, and T32DA07135.*

Tu-AM-J8

THE SERINE CHEMORECEPTOR FROM *ESCHERICHIA COLI* IS METHYLATED IN AN INTERDIMER PROCESS. ((J. Li, J. Wu, G. Li and **R.M. Weis**)) Chemistry Dept. & Program in Molecular & Cellular Biology, University of Massachusetts, Amherst, MA 01003-4510.

The principal site of interaction between the serine & aspartate chemoreceptors (Tsr & Tar) and the methyltransferase (CheR) has been localized to the last five amino acids of the receptor sequence, a site distinct from the sites of methylation. Since the CheR binding motif (NWETF) is not found in all of the methylatable chemoreceptors sequenced to date, the hypothesis was made that receptors are methylated in an interdimer process in which CheR bound to one receptor dimer can catalyze the addition of methyl groups on a neighboring dimer. This hypothesis was tested by a constructing truncated 'substrate subunit' Tsr, which lacked the CheR binding site, but contained the methylatable glutamate (Glu) residues. Significant methylation of substrate subunits was observed only when CheR binding subunit Tsr (full-length Tsr that had the methylation sites blocked by Glu to Gln site-directed mutagenesis) was expressed in the same bilayer membrane. To distinguish between intersubunit-intradimer methylation and interdimer methylation, Tsr substrate subunits were disulfide crosslinked after a D36C mutation was introduced. In the presence of binding subunit Tsr, methyl group incorporation into the crosslinked substrate subunit homodimer was found to be as efficient as the noncrosslinked sample, thus providing strong evidence of the interdimer nature of receptor methylation. These results imply that dimer-dimer interactions play a role in the process of transmembrane signaling.

Tu-AM-J9

LOCAL STRUCTURE AND STRUCTURAL CHANGES IN BACTERIAL CHEMOTAXIS RECEPTORS BY SOLID-STATE NMR ((J. Wang, Y.S. Balazs, E. Del Federico, O.J. Murphy III & **L.K. Thompson**)) Department of Chemistry, University of Massachusetts, Amherst, MA 01003-4510.

The *E. coli* serine receptor binds ligands in the periplasm and transmits a signal across the membrane to modulate phosphorylation reactions which control swimming behavior. Intensive studies of chemotaxis membrane receptors have led to a number of proposals for the molecular mechanism of transmembrane signaling: ligand binding is thought to induce interhelical motions which propagate the signal across the membrane. These proposals can be directly tested with site-directed, solid-state NMR distance measurements on the intact, membrane-bound receptor. We have demonstrated the feasibility of this approach with REDOR measurements on the serine ligand binding site. The 4 Å average distance found between ^{15}N-Ser and the ^{13}CO of two Phe in the binding pocket of the *intact* 120 kDa Ser receptor is consistent with distances predicted from the crystal structure of the periplasmic *fragment* of the related aspartate receptor. Thus, interactions with the ligand amino group are similar for these two receptors and for intact and fragment proteins. Strategies being used to target the experiment to other regions of the receptor include site-directed mutagenesis to introduce unique residues for single-site isotopic labeling. NMR experiments are in progress to *directly* measure interhelical distances and map the motions involved in the transmembrane signaling mechanism.
Supported by NIH (R29-GM47601), NSF (MCB-9258257) and an award from Research Corporation.

Tu-AM-J10

QUANTIFICATION AND DISTRIBUTION OF MEMBRANE PROTEINS STUDIED USING IMAGE CORRELATION SPECTROSCOPY. ((**Claire M. Brown** and Nils O. Petersen)) University of Western Ontario, Chemistry Department, London, Ontario, Canada, N6A 5B7.

Among many other membrane receptors, internalization competent influenza virus hemagglutinin (HA) proteins, interact with clathrin associated adaptor protein (AP-2) via a sorting sequence. Using Image Correlation Analysis (ICS) this study shows that the internalization competent influenza virus hemagglutinin (HA) proteins are more highly aggregated, in the membrane, than the wild type HA, likely due to interactions with AP-2. Two different conditions cause a dispersion of these HA mutants, a decrease in temperature and hypertonic treatment. However, AP-2 distribution is not affected by lower temperatures, but is more disperse with hypertonic treatment. This leads us to believe that the two treatments are causing dispersion of the HA mutants for different reasons, and possible mechanisms for this dispersion will be presented. ICS is a technique which involves a correlation analysis of confocal images of immunofluorescently labelled proteins in the cell membrane. Correlation analysis yields the mean square intensity fluctuation, or the g(0,0) value whose inverse gives a direct measure of the number of independent fluorescent particles (monomers or aggregates) in the observation area. This gives us the ability to quantify proteins within the native membrane and to study the effect of various parameters on the protein distribution.

ION MOTIVE ATPases II

Tu-AM-K1

SCANNING MUTAGENESIS AND DISULFIDE MAPPING OF THE Ca^{2+} BINDING DOMAIN OF SERCA1 ((**W.J. Rice** and D.H. MacLennan)) Banting and Best Department of Medical Research, University of Toronto, Toronto, Ontario, Canada M5G 1L6

Site-directed mutagenesis of SERCA1 has identified six Ca^{2+} binding residues located in transmembrane helices M4, M5, M6 and M8. Scanning mutagenesis of M4 revealed a mutation-sensitive patch on one face of the helix. Scanning mutagenesis has now revealed that M5 and M6 also contain a mutation sensitive face, and a mutation-insensitive, hydrophobic face. Helices M4 and M6 contain a central, six residue motif, E/D–G–L–P–A–T/V, which contains many mutation-sensitive amino acids. M5, which runs antiparallel to M4 and M6, contains the same motif in reverse orientation. These results suggest a sequence duplication between M4 and M6 and convergent evolution of M5 towards this sequence. By contrast, mutagenesis of helix M8 revealed no new mutation-sensitive residues and M8 contains only remnants of the motif. Glu^{908} in M8 remains an outlier among the six Ca^{2+} binding residues.

Our next step in analysis of the Ca^{2+} binding domain is to determine how residues in the active "faces" interact with each other, and with Ca^{2+}, through site-directed disulfide mapping of M4, M5, M6 and M8. Of the 24 naturally-occurring cysteines in SERCA1, 6 lie in the transmembrane domain. Simultaneous replacement of these 6 cysteines reduced Ca^{2+} transport rate to 40% of the wild type activity, without affecting Ca^{2+} affinity. Studies of this mutant have allowed identification of crosslinks between residues in M4 and M6. Since disulfide links also appear to form between cysteines located in the cytoplasmic domain, we are currently removing the remaining cysteine residues before completion of the cross-linking study. (Supported by National Institutes of Health, U.S.A.)

Tu-AM-K2

ABSENCE OF Ca EFFLUX THROUGH PHOSPHOLAMBAN COEXPRESSED WITH SERCA2a. ((Joseph M. Autry and Larry R. Jones)) Krannert Institute of Cardiology, Indiana University School of Medicine, Indianapolis IN 46202

Previously, we have shown that phospholamban (PLB) — purified by sulfhydryl group affinity chromatography or by monoclonal antibody affinity chromatography — induces Ca-selective cation currents when reconstituted into planar lipid bilayers [Kovacs *et al.*, (1988) *J. Biol. Chem.* 263, 18364-18368]. However, it remains unclear whether PLB forms Ca channels in sarcoplasmic reticulum, where PLB regulates the activity of the Ca pump (SERCA2a). To investigate whether PLB forms Ca channels when functionally coupled to SERCA2a, we coexpressed both proteins using the baculovirus expression system. Sf21 cell microsomes containing SERCA2a (no PLB) or SERCA2a plus PLB (PLB expressed at molar excess over SERCA2a) were isolated and actively loaded with Ca in the presence of phosphate. Ca efflux was initiated by chelation of extravesicular Ca with EGTA and monitored in the presence and absence of anti-PLB mAb 2D12, which prevents PLB interactions with the Ca pump. Results (n=4, see below) demonstrate that PLB did not increase Ca efflux from Sf21 microsomes expressing SERCA2a, either with or without addition of PLB mAb. Thus, PLB exhibits no detectable Ca channel activity in Sf21 cell microsomes, when Ca efflux is assayed at zero extravesicular Ca. Experiments are currently in progress to investigate alternative modes by which PLB might form Ca channels, e.g., at µM Ca where the pump remains active.

	Ca Load	Ca Efflux (t=8 min)		Ca Efflux (t=3min)
Proteins Expressed	(nmol Ca / mg)	(nmol Ca / mg) - 2D12	+ 2D12	(nmol Ca / mg) + A23187
SERCA2a	625±35	373±37	362±45	640±19
SERCA2a/PLB	627±61	295±49	298±42	595±48

Tu-AM-K3

RELATIONSHIP BETWEEN INTRINSIC FLUORESCENCE CHANGES AND Ca^{2+} DISSOCIATION FROM SARCOPLASMIC RETICULUM Ca^{2+}-ATPase, IN THE PRESENCE OF KCl or NaCl.

((**Ph. Champeil**)) URA CNRS 2096 & SBPM/DBCM/DSV/CEA, CE Saclay, 91191 Gif-sur-Yvette (France)

Using quin2, a Ca^{2+}-sensitive fluorescent probe and a high affinity chelator, to trigger dissociation of the two Ca^{2+} ions bound to sarcoplasmic reticulum Ca^{2+}-ATPase makes it possible, in a stopped-flow experiment, to monitor under the same conditions both Ca^{2+} dissociation itself, known to be sequential, and the tryptophan fluorescence changes accompanying this dissociation. At pH 6 or 7 in the absence of KCl or NaCl, strictly monoexponential changes in quin2 fluorescence were observed, with exactly the same rate constant as the changes in Ca^{2+}-ATPase tryptophan fluorescence. However, in the presence of KCl or NaCl, the tryptophan fluorescence changes were faster than the still monoexponential quin2 fluorescence changes, and depended on the excitation wavelength. The tryptophan changes apparently monitored the rapid dissociation of the first of the two Ca^{2+} ions to be released from the Ca^{2+}-ATPase; this signal was probably due to tryptophan residues located close to the membrane-water interface and selectable through an appropriate wavelength choice. A slower phase of opposite sign was also detectable in the tryptophan fluorescence changes, presumably related to the dissociation of the second Ca^{2+} ion.

Tu-AM-K4

CHARACTERIZATION OF METAL-BINDING PROPERTIES OF THE N-TERMINAL DOMAINS OF THE MENKES AND WILSON DISEASE PROTEINS.

((**Svetlana Lutsenko**[1], Konstantin Petrukhin[2], T. Conrad Gilliam[2] and Jack H. Kaplan[1])) [1]Dept. Biochemistry and Molecular Biology, OHSU, Portland, OR, 97201; [2]Dept. Psychiatry, Columbia University, New York, NY, 10032. (Spon. by C. Gatto)

N-terminal domains of the Menkes (MNK) and Wilson disease (WD) proteins contains six heavy-metal binding motifs in their sequence. In order to determine the role of N-terminal domains in heavy-metal binding and in the functioning of the MNK and WD proteins these domains have been overexpressed in E.coli as fusions with maltose binding protein. Expressed proteins were purified to homogeneity and their metal-binding properties were determined by metal-chelate chromatography. Both N-terminal domains expressed in water-soluble form bind copper specifically, while proteins obtained after solubilization and refolding of inclusion bodies are less selective and bind copper, zinc and to a lesser extent cobalt. No binding of cadmium was observed. Modification of the expressed domain with a Cys-directed fluorescein coumarin demonstrated that binding of heavy-metals protects Cys-residues against modification. These data suggest that Cys-residues in the N-terminal domain are indeed involved in coordination of heavy-metals. Determination of oxidation state of the copper in the protein complex shows that copper is most likely bound to the N-terminal domains of MNK and WD in a Cu(I) form. Supported by NIH R01 HL30315 to JHK.

Tu-AM-K5

STRUCTURAL CHANGES IN THE NA/K ATPASE FOLLOWING REDOX MODIFICATION OF REACTIVE SULFHYDRYL GROUPS.

((**A.G. Fowler,** *G. Siligardi, D.J. Hearse and M.J. Shattock)) Cardiovascular Research, The Rayne Institute, London SE1 7EH. and *Dept. Pharmacy, King's College, Manresa Road, London SW3 6LX. (Sponsored by M.J. Shattock)

Disturbances of intracellular Na and Ca homeostasis are implicated in ischemia/reperfusion injury in the heart. Electrophysiological study of single cardiac myocytes has shown that oxidative stress, as occurs during ischemia/reperfusion, may inhibit the function of the Na/K pump and contribute to cellular injury. Here we test the hypothesis that key sulphydryl (-SH) groups on the Na/K-ATPase molecule may be targets for oxidation. Such oxidation/blocking may alter the secondary structure and hence the function of the pump protein. Far ultra-violet Circular Dichroism (CD) spectroscopy (wavelength 185 to 260nm) was performed in a Jasco 600 spectralpolarimeter with pure dog kidney Na/K-ATPase (1μM) in **(in mM)** NaCl **30**, KCl 5, $MgCl_2$ 3, ATP **0.1** and Tris **20** (pH7.0). CD spectra were assigned to α-helix, β-sheet plus β-turn and random coil (unordered), using Singular Value Decomposition analysis and seventeen X-ray structures. Certain -SH reactive agents (see fig.) induce a β-domain to α-helix transition in the Na/K-ATPase: specifically, oxidized glutathione (GSSG) altered α-helix content from 53% to 76% at the expense of β-structures and reduced glutathione (GSH) from 53% to 37%.

Changes in cellular redox state and GSH:GSSG during ischemia/ reperfusion may alter the secondary structure of the Na/K-ATPase and may account for oxidation-induced decreases in Na/K pump function and disturbances in ion homeostasis. Key -SH groups on ion translocating proteins may be important therapeutic targets in the treatment of ischemia/reperfusion injury.

Tu-AM-K6

PRE-STEADY STATE ADP AND P_i RELEASE BY Na,K-ATPase.

((E. Buxbaum, T.J.H. Walton and J.D. Cavieres)) Department of Cell Physiology & Pharmacology, Leicester University, P.O. Box 138, Leicester, LE1 9HN, U.K.

We inject [$^3H,\gamma\,^{32}P$]-ATP at 5°C and constant flow rate (≈ 4 ml·s^{-1}) past purified, membrane-bound Na,K-ATPase trapped on a cellulose-nitrate filter. The jet is collected in a rotating 100-cuvette train and nucleotides and P_i are separated by HPLC. Results at 5-20 μM [$^3H,\gamma^{32}P$]-ATP show *simultaneous* bursts of [^3H]-ADP and [^{32}P]-P_i release, the former higher than the latter. The difference largely represents γ-^{32}P-phosphoenzyme (E(P)). ADP and P_i bursts, and the exponential rise of E(P), occur with similar k_{app} = 6-20 s^{-1}. Therefore *i)* E(P) cannot be the precursor of the released P_i and *ii)* there must be an initial rate-limiting step common to ADP release, P_i release, and phosphorylation. At 0.5 μM ATP, however, the ADP burst precedes the P_i burst and E(P) fits the role as P_i precursor (i.e. $dP_i/dt \propto E(P)$). Steady-state measurements of Na,K-ATPase activity at 5°C returned limiting $K_{0.5}$ values < 1 μM and 25 μM. At 5 μM ATP and 5°C, therefore, 18% of enzyme molecules could be initially binding ATP at a low-affinity site, as well as at the high-affinity site. A provisional scheme involves the formation of an E_x-ATP form after reversible ATP binding, followed by 2 branches: 1) ADP release + E(P), and slow E(P) breakdown (the Post-Albers mechanism) and 2) a much faster, apparently-simultaneous ADP and P_i release. The second branch would be activated by ATP binding at a low-affinity ATP site (Ward & Cavieres (1996) J. Biol. Chem. 271, 12317). *Supported by grants from the Medical Research Council and The Wellcome Trust.*

Tu-AM-K7

OSCILLATING ELECTRICAL FIELD-INDUCED INCREMENT IN THE NA/K PUMPING RATE ON SKELETAL MUSCLE FIBERS

((**Wei Chen** and Yu Han)) Department of Surgery, The University of Chicago

Using the improved double Vaseline gap voltage clamp techniques we found strong evidence that Na/K pump current on skeletal muscle cell membrane can be activated by an oscillating electrical field with a defined frequency range. The Na/K pump inhibitors, ouabain and strophanthidine as well as eliminating K ions from the bathing solution were used to identify the Na/K pump currents.

During periods 1 (400 ms) and 3 (200 ms), the membrane potential was held at -90 mV and sampling rate was 500 and 800 us, respectively. An alternative current waveform with a fixed frequency ranged from 100 Hz to 5 kHz was applied to the cell membrane during period 2 (40 ms) with a sampling rate varying from 3 to 30 us depending on the frequency. After subtracting the base line determined by periods 1 and 3, an integration over a number of full cycles of the oscillating transmembrane current in period 2 represents a net transmembrane charges. The integrated net transmembrane charges with ouabain subtracted from those without ouabain is defined as the charges pumped by Na/K pump molecules.

It clearly shows that around 1 ms duration of the external A.C. field, there is a region where the Na/K pump currents were significantly increased. The strength of these studies is not only showing the results, but also the methodology used in the experiments. A simultaneously monitoring changes in pump currents during exposure to an external field dramatically increase the time resolution. This method makes it possible to conduct experiments screening the external field's frequency, magnitude and waveform. (These studies are partially supported by the NIH grant GM50785)

Tu-AM-K8

DOES WHITE NOISE MASK OR ENHANCE THE EFFECTS OF AN ELECTRIC SIGNAL WHICH INDUCES PUMPING OF Rb+ BY Na,K-PUMP?

((T.Y. Tsong[1,2] T.-D. Xie[2], and J.A. Fuchs[2])) 1: Biochem, Hong Kong Univ of Sci & Technology, Kowloon, Hong Kong, and 2: Biochem, Univ of Minn, St. Paul, MN 55108

An important issue in the study of sensual perception is to understand the effects of a high level noise on the reception of a low level signal by an organism. The use of low level electromagnetic fields for studies often produces ambiguous results. Our strategy is to use the electric activation of the Na,K-Pump, which has been characterized in sufficient detail to work out mechanisms of noise effects, and to extend this knowledge to understanding low field effects. White noise with a power spectrum flat between 10 to 100,000 Hz was added to a 1 kHz sinusoidal electric signal for the experiment. A signal at a sub-threshold amplitude (e.g. 10 V/cm) produced little ouabain-sensitive-Rb+ influx in human erythrocytes, but when white noise of an appropriate power level was added, the pump activity was greatly enhanced. This effect diminished at high power levels. Results suggest that noise may enhance the sensitivity of a sensual perception. However, in no cases were the noise enhanced fluxes exceeding the flux induced by an optimal level of signal. Stochastic resonance will be discussed within the framework of the theory of electroconformational coupling to explain these observed effects.

Tu-AM-L1

PIGMENT ORGANIZATION OF BACTERIAL PHOTOSYNTHETIC MEMBRANE AND DYNAMICS OF ENERGY TRANSFER

((**Xiche Hu** and Klaus Schulten)) Beckman Inst., UIUC, Urbana, IL 61801 (Spon. by P. Wolynes)

Structures of all the pigment-protein complexes in the photosynthetic membrane of purple bacteria had been determined except that of light harvesting complex I (LH-I). We have computationally modeled an atomic structure for LH-I of *Rb. sphaeroides* based on a high degree of homology of the αβ heterodimer of LH-I from Rb. sphaeroides to that of LH-II of *Rs. molischianum* [Koepke et al., Structure, 4, 581 (1996)]. The LH-I of *Rb. sphaeroides* is modeled as a hexadecamer of the αβ heterodimers by means of MD simulations and energy minimization. The resultant LH-I structure yields an electron density projection map that is in agreement with the 8.5 Å resolution Electron Microscopy projection map for LH-I of *Rs. rubrum* as reported in Karrasch et al., EMBO J., 14, 631 (1995). A LH-I - RC complex was subsequently formed by energy minimization. Thus, for the first time, a complete picture of pigment organization in the photosynthetic membrane of purple bacteria was achieved at the atomic level. We will first present structural details of all the pigment protein complexes, and then report results of our studies on energy transfer mechanisms based on such pigment organization in two levels: (1) energy transfer within each individual pigment-protein complex; and (2) energy transfer among pigment-protein complexes. In particular, dynamics of exciton transfer from LH-II (through LH-I) to the photosynthetic reaction center will be discussed based on quantum calculations of exciton states of the chlorophyl rings.

Tu-AM-L2

PHOTOELECTRIC AND SURFACE PROPERTIES OF PHOTOSYNTHETIC PIGMENTS IN 2 D

((**R. M. Leblanc**[a], S. Boussaad[a], A. Tazi[a], L. Shao[a], and N. J. Tao[b])) [a]Department of Chemistry, University of Miami, Coral Gables, FL 33124, [b]Department of Physics, Florida International University, Miami, FL 33199

We are investigating the photophysical and photoelectrical properties of electrodeposited and Langmuir-Blodgett (L-B) films of chlorophyll (Chl) *a* in light and in darkness. Scanning tunneling (STM) and atomic force (AFM) microscopic images revealed a change in structure and tunneling spectroscopy revealed a change in the electronic properties. Film grain sizes were found to be larger for illuminated Chl *a* films than the films imaged in darkness. The photovoltaic cells (Al/Chl *a*/Ag cells) exhibited photoelectric properties that are film structure dependent. In the monolayer L-B films of Chl *a*, the STM and AFM images present a dimeric form of Chl *a* with an average size of 3.00 ±0.15 nm. The Chl *a* monolayers mimic the pigment packing *in vivo*. We investigated the light energy conversion efficiency of Chl *a* L-B film on SnO_2 optically transparent electrode, and absorption and fluorescence properties at air-water interface. Spectra of photocurrents coincided with the absorption of Chl *a* in mono-and multilayers at SnO_2/electrolyte interface. We have also recorded the topographical images of photosystem II using STM and AFM. AFM recordings of PSII images in tapping mode revealed some interesting features. The data on STM and AFM images of PSII will be discussed.

Tu-AM-L3

REACTION ORDER AND THERMODYNAMICS OF *RHODOBACTER SPHAEROIDES* LH1 COMPONENTS: β PEPTIDE DIMERIZATION IN MICELLES.

((**R. D. Krueger-Koplin**, C.C. Schenck))Department of Biochemistry and Molecular Biology, Colorado State University, Fort Collins, CO 80523-1870.

The β-peptide from light-harvesting complex 1 (LH1) binds bacteriochlorophyll *a* (BChl*a*) noncovalently in β-octylglucoside (βOG) detergent micelles to form a species called β-B777, with absorbance maximum at 777nm. β-B777 oligomerizes to form a spectrally-defined complex (β-B824) with maximal absorbance at 824 nm when the micelle concentration is reduced. Dilution below the critical micelle concentration for βOG yields a novel species β-B926. The figure shows the log-log absorbance relationship of BChl*a* species at 777 and 824nm upon dilution with buffer at constant βOG concentration (4.4% βOG, initial BChl*a* and β peptide concentrations 250μM) . The slope of 2.0 represents the oligomerization reaction order for formation of β-B824 from β-B777, suggesting that the β-B820 complex is formed by the association of 2 β-B777s, giving rise to a β_2BChl_2 dimer (β/β-B824).

The formation of β/β-B824 from β-B777 proceeds with a well-defined isosbestic point and is fully reversible, allowing us to determine K_{eq}^{app} for the dimerization. The temperature dependence of the associative equilibrium 2 β-B777⇌β/β-B820 favors complex formation at lower temperatures. By measuring the relative concentrations of the two species over the temperature range 4 to 37°C, $\Delta H^{o,1\%\,\beta OG}$ and $\Delta S^{o,1\%\,\beta OG}$ of association for β/β-B824 are determined to be -62 kJ·mol^{-1} and -0.12 kJ·mol^{-1}·K^{-1}, respectively. Support by NIH GM48254 and CIRB.

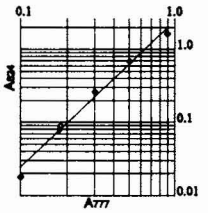

Tu-AM-L4

STUDY OF SYMMETRY-RELATED MUTANTS IN THE QUINONE BINDING SITES OF *RHODOBACTER CAPSULATUS* REACTION CENTERS

((M. Valerio-Lepiniec[1], M. Schiffer[2], **P. Sebban**[1] and D.K. Hanson[2])) [1]CGM, C.N.R.S., 91198, Gif, FRANCE; [2]CMB, Argonne Natl. Lab., Il., USA.

Absorption of light by photochemical reaction centers (RCs) results in coupled electron and proton transfers involving primary (Q_A) and secondary (Q_B) quinone acceptors. In bacterial RCs of *Rb. capsulatus*, we have constructed a family of site-specific mutants where two important groups for proton delivery to Q_B have been mutated to non-protonatable groups (L212Glu→Ala, L213Asp→ Ala) and conversely, the symmetry-related groups in the Q_A binding pocket have been mutated to protonatable residues (M246Ala→Glu, M247Ala→Asp). The resulting quadruple mutant (RQ) is incapable of photosynthetic growth. Activity is restored in spontaneous phenotypic revertants by second-site mutations affecting Q_B function which are coupled to mutations near Q_A that restore an Ala or substitute a Tyr at the original M247 site; one strain carries an additional Met→Leu substitution at M260 near Q_A. Time resolved-spectroscopy of the RCs from these strains reveals that the compensating mutations at the Q_B site [distant (≈ 10-15 Å) from Q_B] accelerate the electron and proton transfer rates compared to the RQ mutant. However, these rates as well as the overall cycling process of the RCs mutated in both the Q_A and Q_B pockets remain more than one order of magnitude slower than those observed in the WT and in the mutants which carry a wild-type Q_B pocket. Interestingly, the engineered M246Ala→Glu substitution located nearby Q_A affects only the binding of this acceptor, but not the electron transfer capabilities of the RCs. Supported by Human Frontier of Science collaborative grant RG329-95, U.S. Dept. of Energy/OHER, contract No. W-31-109-ENG-38 and by U.S. PHS GM36598.

Tu-AM-L5

EFFECT OF THE INTERDOMAIN BASIC REGION OF CYTOCHROME *f* ON ITS REDOX REACTIONS *IN VIVO*

((**G. M. Soriano**, M. V. Ponamarev, G.-S. Tae, and W. A. Cramer)) Department of Biological Sciences, Purdue University, W. Lafayette, IN 47907. (Spon. by R. A. Dilley)

The prominent interdomain basic surface region seen in the high resolution structure of the lumen-side C-terminal fragment of turnip cytochrome *f*, containing the conserved Lys58,65,66 (large domain) and Lys187 (small domain), has been inferred from *in vitro* studies and modeling to be responsible for docking of its oxidant, plastocyanin. The effect of the putative docking region of cyt *f* on its reactivity *in vivo* was tested by mutagenesis in *C. reinhardtii*. Three charge-neutralizing mutants were constructed involving: (i) the 2 lysines (Lys188Asn-Lys189Gln) in the small domain, (ii) the 3 lysines (Lys58Gln-Lys65Ser-Lys66Glu) in the large domain, and (iii) all 5 of these lysines. All mutants grew phototrophically. The mutants displayed a 25% increase in generation time, and comparable decreases in rates of O_2 evolution and the slow electrochromic band shift. The changes were largest in the five-fold Lys-minus mutant (Lys58Gln-Lys65Ser-Lys66Glu-Lys188 Asn-Lys189Gln). The mutants showed a small increase (~ 25%) in the $t_{1/2}$, from 0.2 to 0.25 msec, of cyt *f* photooxidation, far less than anticipated (ca. 100-fold) from *in vitro* studies of the effect of ionic strength on the cyt *f*-PC interaction.

Cells grown without Cu, where cyt c_6 replaces PC as the electron acceptor of cyt *f*, displayed rates of cyt *f* photooxidation slightly faster than those grown with Cu, but which also decreased by ~25% in the Lys-minus mutants.

It was concluded that the net effect of electrostatic interactions between cytochrome *f* and plastocyanin *in vivo* is much smaller than that measured *in vitro* and is not rate-limiting. This may be a consequence of a relatively high ionic strength environment and the small diffusional space available for collision and docking in the internal thylakoid lumen of log phase *C. reinhardtii*. [NIH GM38323].

Tu-AM-L6

THE CRYSTALLIZATION AND STRUCTURE OF A SOLUBLE FORM OF *Chlamydomonas reinhardtii* CYTOCHROME F .

((E.A. Berry, L-s. Huang, Y. Chi, Z. Zhang, R. Malkin* and J. G. Fernandez-Velasco*)) Calvin Lab and (*)Dept. Plant Biology, Univ. of California. Berkeley, CA 94720. (Spon. by A.J. Bearden)

The cytochrome f of *C. reinhardtii* is highly homologous to the turnip one, for which the structure of a soluble form is known (1,2). As *C. reinhardtii* is a preferred system to study function of the electron transfer chain using site directed mutagenesis, the determination of the actual structure of this cytochrome for the microalga is of high interest. A carboxy terminus truncated, soluble form of cytochrome f from *C. reinhardtii* F283ST (3) was purified to homogeneity and crystallized in space group P212121 with unit cell parameters 76.4, 94.9 and 120.2 Å. An X-ray diffraction data set was collected to 2.2 Å, and phased by molecular replacement using the published structure from turnip as a model (1). The asymmetric unit contains a trimer, so three structures of the molecule in different crystallographic environments were obtained. Comparison of the three monomers with each other and with the turnip structure shows which parts of the molecule are flexible and which features (such as bound ions or water) are variable. Although superimposing the core of the large domain of the 3 monomers and the turnip structure shows some flexibility in the interdomain hinge and in several loops, the structure of both species are very similar. In particular the features recognized in (1,2): the hydrophobic outer face of the heme binding pocket with Y1 parallel to the heme plane, the cluster of lysines 58,65,66,188 and189 (as putative plastocyanin binding site) and the chain of 5 waters between the heme and K66 are present in all 3 monomers. It is of interest that, as in turnip, the lateral chain of K66 points away of the K cluster and that K207, unlike its sequence counterpart R209 in turnip, is out of the K cluster.

1) Martinez, SE; Huang, D; Szczepaniak, A; Cramer, WA and Smith, JL (1994) Structure 2, 95. 2) Martinez, SE; Huang, D; Ponomarev, M; Cramer, WA and Smith, JL (1996). Protein Science 5, 1081. 3) Kuras, R; Wollman, F-A and Joliot, P (1995) Biochemistry 34, 7468.

Tu-AM-L7

THE PUTATIVE PLASTOCYANIN BINDING SITE IN *Chlamydomonas reinhardtii* CYTOCHROME F . ((J.G. **Fernandez-Velasco**, J. Zhou and R. Malkin)) Dept. Plant Biology, 461 Koshland Hall. Univ. of California. Berkeley, CA 94720.

The cluster of lysines proposed as the plastocyanin binding site in the cytochorome f of turnip (1) has a similar configuration in *C. reinhardtii* (2). Mutants of *C. reinhardtii* were prepared with altered electrical charge for lysines 58, 65, 66 (large domain) and 188, 189 (small domain) and the photooxidation of cyt f was measured. The reaction t1/2 for the wt is 0.20 ms (in the presence of stigmatellin and ionophores, at pH 7.0, Eh 0 mV, low ionic strength and 25°C). The reaction t1/2 for a first series of mutants analyzed are a) L188/L189 (0.38 ms), b) L188/L189/E58 (1.5 ms), c) L188/L189/E65 (2.2 ms), d) L188/L189/E66 (1.0 ms), e) E65/E66 (0.65 ms), f) E58/E65/E66 (1.5 ms), g) L188/L189/E65/E66 (2.1 ms) and h) L188/L189/E58/E65/E66 (1.5 ms). In all cases error is ca. $\leq \pm$ 15%. In contrast, the rates of cytochrome f re-reduction are very similar (t1/2 3-5 ms) in wt and all mutant strains. It is concluded that: 1) Lys residues from both the small and large domains are involved in the cytochrome fast oxidation but not, or only marginally, in the re-reduction from the FeS center. This is in agreement with the expected role for the altered amino acid residues as participants in the binding/electron transfer to plastocyanin. 2) All three Lys in the large domain are involved but they are not equivalent. 3) Synergistic effects between both domains exist, cf. a, e and g. 4) The degree of inhibition saturates by increasingly diminishing the net positive charge of the cluster. A reaction with t1/2 ca. 2.2 ms is the slowest attainable by neutralizing/inverting the cluster's positive charge complement. This could be explained either by a structural change of the site in the polymutated strains (cf. c vs. g and h), driven by the accumulation of Glu or by the elicitation of an alternative independent (artifactual?) reaction mechanism with plastocyanin. 1) Martinez, SE; Huang, D; Szczepaniak, A; Cramer, WA and Smith, JL (1994) Structure 2, 95-105 2) Berry, EA; Huang, L-s; Chi, Y; Zhang, Z; Malkin, R and Fernandez-Velasco, JG, this Meeting.

STRUCTURAL DETERMINANTS OF CALCIUM CHANNEL SIGNALING

T-PM-SymI-1 **W. Catterall, University of Washington**
Presynaptic Calcium Channels: Modulation and Role in Transmitter Release

T-PM-SymI-2 **T. Snutch, University of British Columbia**
Cross-talk Between PKC Up-regulation and G-protein Down-regulation of Calcium Channels

T-PM-SymI-3 **K. Campbell, University of Iowa**
Subunit Interaction Sites in Voltage-gated Calcium Channels

T-PM-SymI-4 **K. Beam, Colorado State University**
Cross-talk Between Voltage-gated and Intracellular-release Calcium Channels

AIDS AND ITS ASSOCIATED OPPORTUNISTIC INFECTIONS - DRUG DISCOVERY AND DEVELOPMENT

T-PM-SymII-1 **H. Ukwu, Merck Research Laboratories**
Anti-HIV Drugs - U.S. Regulatory Process

T-PM-SymII-2 **M. A. Navia, Vertex Pharmaceuticals, Inc.**
Structure-based Drug Design of HIV Protease Inhibitors - Tolerability, Bioavailability and Potency as Design Criteria

T-PM-SymII-3 **J. Sacchettini, Texas A&M University**
Alternative Strategies for Combatting Multi-Drug Resistance in Tuberculosis

T-PM-SymII-4 **D. R. Davies, NIDDK**
Structural Studies of the HIV Integrase